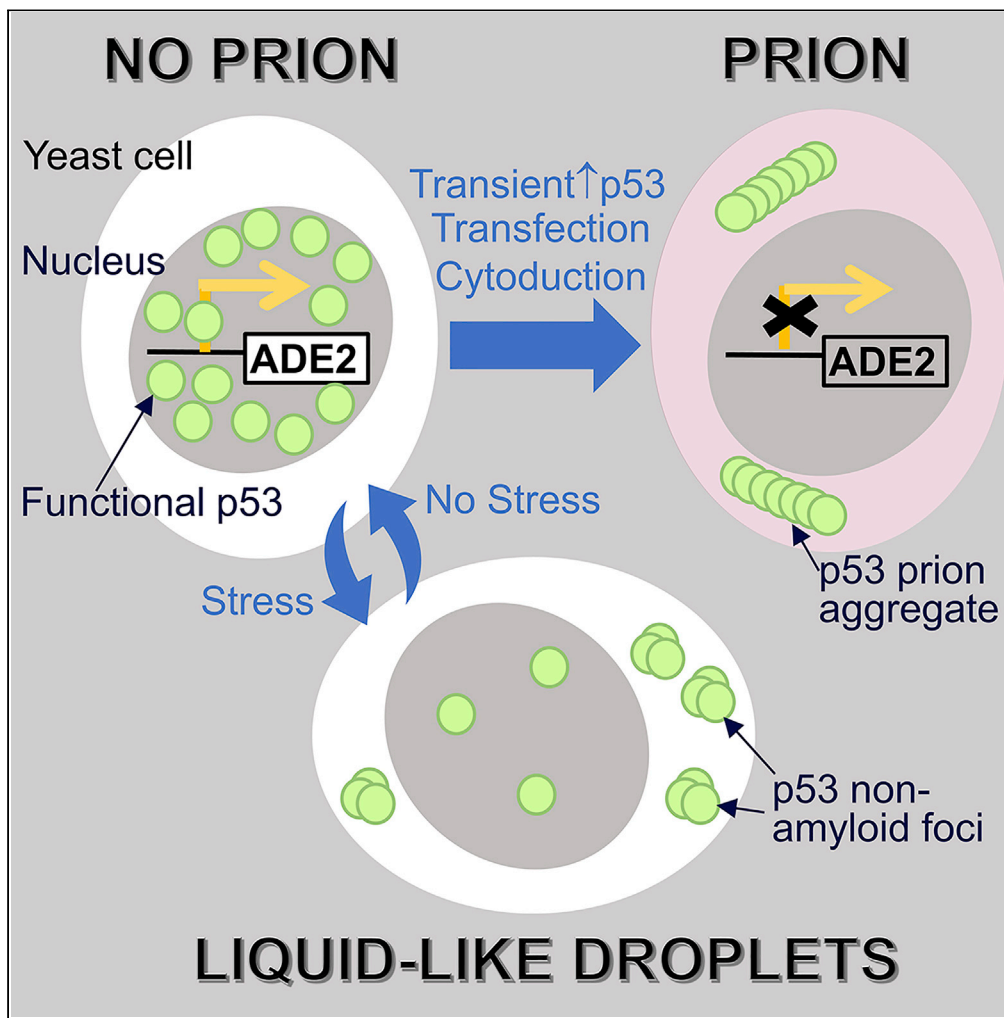**Article**

Tumor suppressor protein p53 expressed in yeast can remain diffuse, form a prion, or form unstable liquid-like droplets

Sei-Kyoung Park,
Sangeun Park,
Christine Pentek,
Susan W. Liebman

sliebman@unr.edu

HIGHLIGHTS

A published yeast model of functional nuclear human p53 tumor suppressor was used

Upon transient overexpression p53 loses its transcription function and aggregates

These p53 aggregates are cytoplasmic and behave like stable heritable prions

Stress induces p53 to form liquid-like droplets that are unstable and not prion-like

iScience

Article

Tumor suppressor protein p53 expressed in yeast can remain diffuse, form a prion, or form unstable liquid-like droplets

Sei-Kyoung Park,[1] Sangeun Park,[1] Christine Pentek,[1] and Susan W. Liebman[1,2,*]

SUMMARY

Mutations in the p53 tumor suppressor are frequent causes of cancer. Because p53 aggregates appear in some tumor cells, it has been suggested that p53 could also cause cancer by forming self-replicating protein aggregates (prions). Here, using yeast, we show that transient p53 overexpression induced the formation of p53 prion aggregates that were transmitted for >100 generations, found in lysate pellets, stained with Thioflavin T, and transmitted by cytoplasmic transfer, or transfection with lysates of cells carrying the prion or with p53 amyloid peptide. As predicted for a prion, transient interruption of p53 expression caused permanent p53 prion loss. Importantly, p53 transcription factor activity was reduced by prion formation suggesting that prion aggregation could cause cancer. p53 has also been found in liquid-like nuclear droplets in animal cell culture. In yeast, we found that liquid-like p53 foci appear in response to stress and disappear with stress removal.

INTRODUCTION

Mutations in the human p53 transcription factor are a frequent cause of cancer. Cancers occur when a normal cell undergoes a series of mutations that transform it into a cell that grows without control. The most important tumor suppressor gene is likely the p53 transcription factor dubbed the "guardian of the genome" and "policemen of the oncogenes" (Lane, 1992; Levine and Oren, 2009; Levine et al., 2011; Ozaki and Nakagawara, 2011). Indeed, in more than 50% of human cancer cells, at least one of the two p53 alleles carries a mutation. Furthermore, people born without p53 always get cancer (Iwakuma et al., 2005).

It has been hypothesized that inactivation of p53 leading to tumor formation may be caused not only by mutations in p53 but also when p53 forms punctate inclusions that have been seen in tumor cell lines and cancer biopsies with certain p53 mutations (reviewed in de Oliveira et al., 2020; Navalkar et al., 2020). Interestingly, these puncta have some of the biochemical characteristics of amyloid, which is found in many prion aggregates. Also, certain mutant p53 can form fibers *in vitro* that stain with dyes suggestive of amyloid (Congo red and Thioflavin T [ThT]) and have an X-ray diffraction characteristic of amyloid. Although the kinetic properties of p53 aggregation *in vitro* are not equivalent to classic nucleated growth expected of amyloid (Wilcken et al., 2012), wild-type p53 aggregation can be stimulated by the addition of mutant p53 fibers (Ano Bom et al., 2012).

Furthermore, a p53 peptide of eight residues (amino acid [aa] 250–257, PILTIITL called P8) forms amyloid fibers *in vitro* and seeds the formation of a larger "core" domain of p53 (aa. 94–312) to form amyloid. Fibers of this peptide, when internalized by SH-SY5Y neuroblastoma cells, caused the appearance of intracellular p53 aggregates, and lysates of these cells internalized by virgin cells caused *de novo* p53 aggregation (Ghosh et al., 2014, 2017). Thus p53 aggregates can enter cells and seed aggregation of endogenous p53. However, this could occur if intra-cellular p53 decorates the infecting aggregates as has been seen for prion-like proteins such as Huntingtin that do not form heritable prions (Osherovich et al., 2004).

Real prion formation also requires that the newly aggregated p53 fragments in the cell create an exponential increase in propagon number that can then infect other cells. The goal of this work was to determine if

[1]Department of Pharmacology, University of Nevada, Reno, NV 89557, USA

[2]Lead contact

*Correspondence: sliebman@unr.edu

p53 can form such a prion and, importantly, if this is associated with loss of p53 function, which would likely cause cancer.

Prions are altered conformations of a protein that seed other molecules of that protein to rapidly adapt the prion conformation. At a given concentration in the cell these proteins remain soluble in the absence of seed but aggregate in the presence of seed. What causes the occasional *de novo* switch from a soluble protein to a prion seed in the absence of an infecting propagon is largely unknown. Once formed, however, prion aggregates increase in number when they fragment creating new seeds with ends that attract and template soluble conformers of that protein to rapidly switch to the prion conformation. Importantly, only a limited number of proteins, which generally have unstructured domains, are able to form amyloid *in cells*, even though all proteins can misfold into an amyloid conformation under non-physiological conditions (Chiti and Dobson, 2006). Furthermore, not all proteins that form amyloid in cells fragment to form heritable prions (Caudron and Barral, 2013; Marchante et al., 2017).

Prions have been found in yeast where they control endogenous traits (Liebman and Chernoff, 2012). These yeast proteins can lose, or change, their function when they switch to an aggregated, often amyloid conformation. Studies of prion proteins in yeast have contributed much to our knowledge about this phenomenon in human disease (Armakola et al., 2011; Bagriantsev and Liebman, 2006; Bonini and Gitler, 2011; Chernoff et al., 1995; Liebman and Chernoff, 2012; Park et al., 2011; Treusch et al., 2011). Indeed, the prion hypothesis was first proved when transfection of prions, in the form of pure amyloid fibers, into yeast cells caused prion infection transmitted for many generations (King and Diaz-Avalos, 2004; Tanaka et al., 2004). Interestingly, the majority of yeast prions and human disease proteins with prion-like domains are, like p53, nucleic acid-binding proteins (March et al., 2016).

Although yeast do not have endogenous p53, a robust assay for transcription factor activity of human p53 expressed in yeast has been used for decades (Fronza et al., 2000; Inga et al., 1997; Monti et al., 2019). High-level expression of wild-type p53 has been shown to cause reduced growth of some yeast strains under certain growth conditions. As loss-of-function p53 mutants did not have this effect, it was suggested that the growth inhibition is caused by the functional p53's aberrant transcription of endogenous yeast genes (Bischoff et al., 1992; Inga and Resnick, 2001; Kumar et al., 2017; Nigro et al., 1992). Thus, we reasoned that inactivation of p53 by prion formation might reduce its ability to inhibit growth.

Transient overexpression of yeast prion proteins induces the proteins to form aggregates that are self-seeding and efficiently fragment, so they propagate even after overexpression is removed (Alberti et al., 2009; Byers and Jarosz, 2017; Chakrabortee et al., 2016; Chakravarty et al., 2020; Derkatch et al., 1996; Du et al., 2008; Harvey et al., 2020; Itakura et al., 2020; Liebman and Chernoff, 2012; Patel et al., 2009; Wickner, 1994). Thus, transient overexpression of mutant or wild-type p53 could increase the likelihood of *de novo* p53 prion formation and inactivation, leading to a chain reaction of p53 aggregation and aggregate replication. This could explain why inactive wild-type p53 is found in the cytoplasm of some tumors (Elledge et al., 1994; Moll et al., 1995, 1997) and why melanoma cells expressing high levels of wild-type p53 are often associated with inactive p53 (Houben et al., 2011).

In addition to forming aggregates that are amyloid-like, p53 has also been shown to be present in non-membrane-bound liquid-like nuclear droplets, including Cajal and promyelocytic leukemia protein bodies (Banani et al., 2017; Cioce and Lamond, 2005; Fogal et al., 2000; Guo et al., 2000). p53 can also form liquid-like droplets *in vitro* (Kamagata et al., 2020). Other proteins with disordered sequences capable of forming amyloid aggregates can also form cellular and *in vitro* liquid-like droplets under certain conditions. These droplets appear to form by liquid-liquid phase separation (LLPS). Unlike amyloid-like prion aggregates, liquid droplets are not stable. They often appear and disappear in the cell in response to protein-specific stress triggers (Boeynaems et al., 2018; Boncella et al., 2020; Buchan et al., 2011; Chakravarty and Jarosz, 2018; Grousl et al., 2013; Itakura et al., 2018; Jin et al., 2017; Lee et al., 2018; Narayanaswamy et al., 2009). In particular, P-bodies, highly conserved RNA-protein granules that increase in number to help cells divert resources to survival in response to stress, have been shown to be liquid-like droplets in yeast (Kroschwald et al., 2015). Although the relationship between liquid droplets and amyloid aggregates is unknown, it has been suggested that the temporary concentration of a protein with an unstructured domain into a liquid droplet may enhance its chance of forming a more stable prion-like aggregate (Boeynaems et al., 2018; Taylor et al., 2016).

Here, we show that wild-type human p53 expressed in yeast and normally found to be diffuse in the nucleus can be induced to form cytoplasmic foci of two types. Transient overexpression of p53 resulted in the appearance of stable transmissible prions with amyloid-like structure, whereas the stresses of ethanol, heat, or glucose starvation caused the appearance of unstable non-amyloid foci.

RESULTS

Establishment of a yeast strain with stable p53 cytoplasmic foci

We obtained stable heritable aggregates of p53 by screening for isolates with impaired p53 activity and increased p53 aggregation, following transient overexpression of p53. We used strain yIG397, containing an *ADE2* reporter controlled by a promoter that is dependent upon p53 binding, and is therefore diagnostic for functional p53 activity (Inga et al., 1997). To obtain strain L3671, in which p53 expression could be controlled, yIG397 was co-transformed with a *CEN* plasmid constitutively expressing untagged wild-type p53 driven by the constitutive *ADH* promoter (pADH1-p53), as well as with a *CEN* plasmid expressing p53-EYFP from an inducible *GAL* promoter (pGAL-p53-EYFP). L3671 showed the expected *ADE2* reporter phenotypes for functional non-prion wild-type p53: cells were white, indicative of full *ADE2* expression resulting from p53 activity. We expected cells with a prion form of p53 to have reduced p53 function due to aggregation, resulting in reduction of *ADE2* expression leading to reduced growth and a red or pink color on adenine-limiting media (Figure 1A).

L3671 cells grown on galactose, to overexpress p53-EYFP, or glucose, as control, were transferred to glucose medium with limiting adenine to end the p53-EYFP expression (see Transparent Methods for details). As untagged p53 was still expressed from the *ADH1* promoter, these cells were expected to remain white unless the p53 activity was reduced, e.g., by forming a prion. A few small dark red colonies were seen whether the cells were previously grown on glucose or galactose. These colonies were all [*rho*⁻], which frequently arise in yeast cultures due to the loss of functional mitochondria. However, on the plates that were replica-plated from galactose, but not from glucose, there were also larger pink colonies. Cells from 25 such colonies were patched and replica-plated to glucose media along with non-prion control L3671 that had never been grown on galactose (Figure 1B).

To visualize aggregation of p53, the L3671 control and five of the pink derivatives were grown on galactose to allow expression of the p53-EYFP. In control cells p53-EYFP was generally diffuse in nuclei (Figure S1), with less than 1% of the cells containing cytoplasmic fluorescent dots. In contrast, fewer of the pink cells had p53 in nuclei and many had cytoplasmic fluorescent dots. Nuclear fluorescent foci were seen in some preparations but were hard to reliably distinguish from control nuclei. To determine if the elevated presence of cytoplasmic dots was stable, we sequentially subcloned and repeatedly patched one of these isolates (#7, named L3672 prion subclone) on plasmid-selective glucose media for over 100 generations and they remained pink, indicative of prion retention (Figure 1C). Also, even in the presence of adenine, the prion subclones grew slower than the non-prion control (Figure 1C), an effect frequently seen for other prions and prion-like aggregates (Armakola et al., 2011; Liebman and Chernoff, 2012; Park et al., 2017; Pezza et al., 2014).

We then grew the white L3671 (non-prion control) and pink L3672 (prion subclones) on galactose medium to induce p53-EYFP and found that <1% of the non-prion control cells had cytoplasmic dots and >99% had nuclear, generally diffuse, p53-EYFP, excluding dead cells, cells that had no fluorescence, and cells that *only* had fluorescence in the vacuole. In contrast, about 30%–50% of cells in the prion subclones had cytoplasmic dots and only about 70%–50% had nuclear p53-EYFP (Figure 1E). Finally, many of the cells in the prion cultures had fluorescence only visible in the vacuole.

Yeast prion aggregates, e.g., [*PSI*⁺] and [*PIN*⁺], are stained by ThT, which causes them to fluoresce with a CFP filter (Arslan et al., 2015; Summers and Cyr, 2011). Likewise, ThT stains aggregates of the amyotrophic lateral sclerosis-associated human proteins FUS and CREST, but not TDP-43, when expressed in yeast (Park et al., 2019). Figure 1F shows that the p53-EYFP cytoplasmic foci present in L3672 are stained by ThT. This is not caused by bleed through from the p53-EYFP, because in the absence of ThT no such CFP fluorescence is visible. This staining suggests that the cytoplasmic p53-EYFP aggregates are amyloid-like, a characteristic of many prions.

Furthermore, when the prion subclones, which showed p53-EYFP fluorescent aggregates on galactose, were transferred to glucose where only the untagged p53 is expressed, ThT staining still revealed the
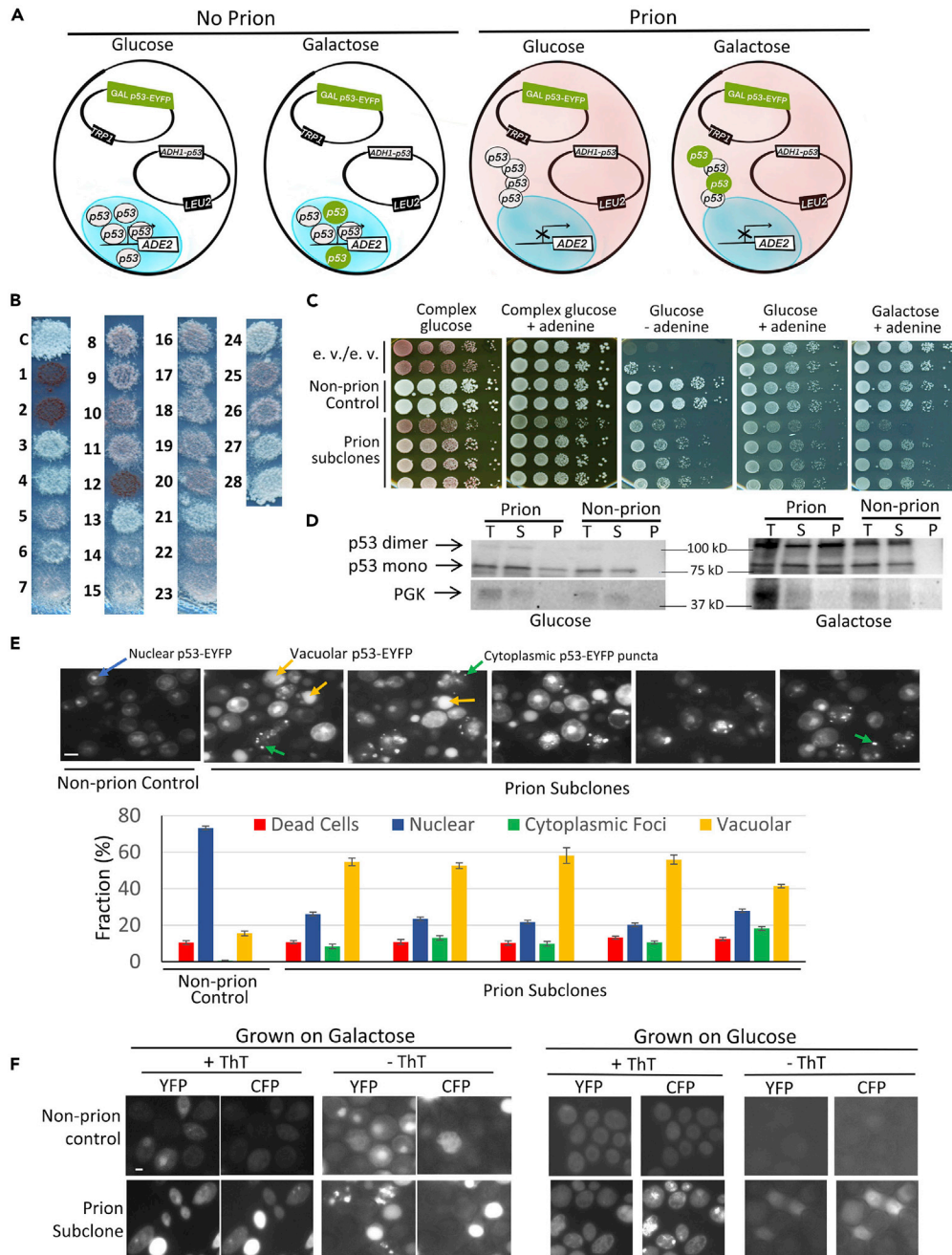
Figure 1. Wild-type p53 forms stable cytoplasmic aggregates that reduce p53 activity

(A) *Cartoon of strain L3671 in which prion candidates were obtained showing cells with and without prion grown on glucose versus galactose.* Shown are plasmids p*ADH1-p53* and p*GAL1-p53-EYFP* and *ADE2* reporter gene under p53 control, contained in L3671. The nucleus is depicted as a blue oval. Even though the plasmids are nuclear, they are shown in the cytoplasm to make it easier to see them. In the absence of prion, p53 is in the nucleus where it is diffuse and turns on the *ADE2* gene, making cells white and able to grow in the absence of adenine. In the presence of prion, p53 forms cytoplasmic puncta, reducing the amount of p53 in the nucleus so that *ADE2* is not transcribed efficiently, and the cells are reddish in color on most media and grow poorly in the absence of adenine. L3671 grown on glucose only expresses untagged p53, from the constitutive *ADH1* promoter. L3671 grown on galactose also expresses p53 tagged with EYFP from the *GAL1* promoter. The nuclei in cells without the prion grown on galactose (but not glucose) show diffuse green fluorescence. Likewise, the cytoplasmic p53 foci in prion cells are only fluorescently tagged when grown on galactose.

Figure 1. *Continued*

(B) *p53 prion candidates have reduced p53 activity.* Cells shown are on plasmid-selective, adenine-limiting, glucose medium. The L3671 control (C) and prion candidates (1–28) are shown. Reduced expression of *ADE2*, and therefore reduced p53 activity, is seen as a pinkish color and reduced growth on media with limited adenine. Expression of p53 cannot be estimated in candidates 1, 2, or 12, because they are [*rho⁻*] and this loss of mitochondria caused them to become dark red.

(C) *Reduced ADE2 expression is stably maintained in a p53 prion candidate.* Following extensive culturing, normalized suspensions of subclones of prion candidate #7 (L3672), non-prion control (L3671) and empty vector (e.v.) control strain (yIG397), were one-tenth serially diluted in water and spotted on YPD (complex glucose) with and without additional adenine, on plasmid-selective synthetic glucose (glucose) with and without adenine, and on plasmid-selective 2% galactose medium with adenine plates. These plates were photographed after 3–5 days of incubation at 30°C. Red papillations on the non-plasmid-selective YPD plate without excess adenine result from loss of the p53 plasmid.

(D) *p53 sediments more in lysates of prion candidates than in non-prion controls.* Non-prion control (L3671) and prion (L3672) cells grown in plasmid-selective glucose or galactose media were lysed as described in Transparent Methods. Total lysates (T) were separated into Supernatant (S) *and* Pellet (P) by centrifugation at 80K RPM for 30 min. Samples were run on SDS-PAGE, and gels were immunoblotted with anti-p53, stripped, and reprobed with anti-PGK for a loading control. Detection of p53-EYFP monomer (~70 kD) or dimer and PGK (44.7 kD) on western blot was based on migration of Precision Plus Protein Dual Color (Bio Red, Hercules, CA).

(E) *Prion candidate has p53-EYFP cytoplasmic foci.* Both non-prion control (L3671) and prion candidate (L3672) repeatedly subcloned cells, grown on galactose to induce expression of *GAL1-p53-EYFP,* were examined under a fluorescent microscope and photographed (top). The fraction of cells with nuclear fluorescence (Nuclear), cytoplasmic aggregates (Cytoplasmic Foci), or vacuolar fluorescence (Vacuolar) was determined, counted, and converted into % fraction (bottom). Trypan blue was used to stain dead cells. Standard error of the mean bars shown were based on nine replicates and 200–700 cells were scored for each replica. The prion and non-prion cultures were statistically different (p < 0.05%) for fractions of cells with nuclear fluorescence, cytoplasmic puncta, and vacuolar fluorescence.

(F) *p53 prion-like aggregates stain with Thioflavin T.* Fluorescence of non-prion control (L3671) and prion cells (L3672) both containing p*ADH1-p53* and p*GAL1-p53-EYFP* grown on plasmid-selective galactose (left) or glucose (right) plates, fixed and stained (+ThT) or not stained (- ThT) with Thioflavin T versus EYFP fluorescence were, respectively, detected under CFP versus YFP filters. Cells expressing EYFP that were stained with Thioflavin T exhibited reduced, but detectable, EYFP fluorescence. Scale bar, 5 μM. Note: dead cells often look bright due to increased autofluorescence.

See Figures S1 and S2 for additional characterization of p53 non-prion and prion strains and Tables S1 and S2 for a description of strains and plasmids.

presence of amyloid-like cytoplasmic foci (Figure 1F). This suggests that the p53-EYFP aggregates were prions that seeded the untagged p53 to also form amyloid-like prion aggregates. Also as predicted, when control cells that showed mostly nuclear diffuse p53-EYFP on galactose, were transferred to glucose, ThT staining did not reveal cytoplasmic foci. Nuclei, even if shown to contain p53-EYFP, never stained with ThT in either control or prion-containing cells. This suggests that unlike the cytoplasmic p53 aggregates, the p53 in nuclei is not amyloid-like.

One of the hallmarks of prion aggregation in yeast is the conversion of a soluble protein to one that is found in the pellet when lysates are centrifuged (Liebman and Chernoff, 2012). Likewise, we found that p53 is soluble when expressed in yeast in the non-prion form but is largely found in the pellet in cells with the p53 prion (Figure 1D). Another hallmark of prions in yeast is dependence on chaperones. Most but not all yeast prions are dependent on the presence of the HSP104 chaperone that is not found in mammals (Liebman and Chernoff, 2012). Other yeast prions have been shown to be dependent on HSP90 (Chakrabortee et al., 2016). We found that neither 5 mM guanidine hydrochloride, which inactivates the HSP104 chaperone, nor deletion of *HSP104* cured cells of the p53 prion (Figures S2A and S2B). Likewise addition of radicicol, which inactivates HSP90 (Sharma et al., 1998), did not cause loss of the p53 prion (Figure S2C).

Wild-type p53 cytoplasmic aggregates can be transferred by cytoduction to both wild-type and R175H mutant p53

Cytoduction was used to transfer cytoplasm from the *MATα* [*RHO⁺*] donor control (L3671) and isogenic p53 prion subclones (L3672) to *MAT***a** *kar1* [*rho⁻*] recipient cells constitutively expressing p53-EYFP or p53-R175H-EYFP, which contains a cancer hotspot structural mutation. Before cytoduction, fluorescence in these recipient cells was largely diffuse in nuclei, but occasional cytoplasmic dots were more frequently seen in p53-R175H-EYFP versus p53-EYFP cells. The *kar1* mutation prevents nuclear fusion so buds from the zygote with the recipient nucleus and mixed cytoplasm "cytoductants" can be selected (Conde and Fink, 1976) (Figure 2A). Cytoductants were identified because they were [*RHO⁺*], and therefore have donor cytoplasm, but have the unique auxotrophic markers and mating type diagnostic of the recipient. We then
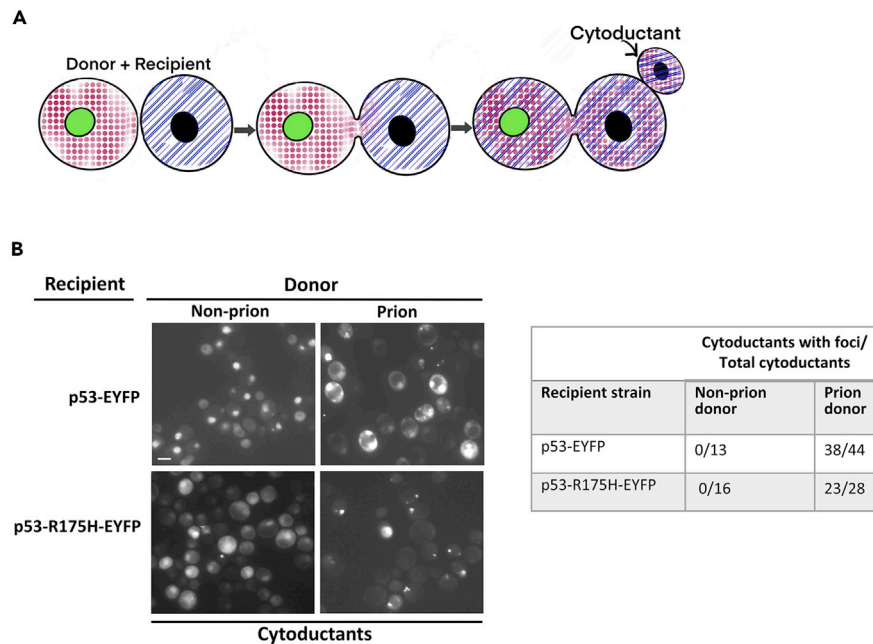
Figure 2. p53 prion-like aggregates can be transferred by cytoduction, from prion donor cells, to non-prion recipient cells expressing either wild-type p53 or mutant p53-R175H

(A) *Cartoon illustrating cytoduction.* Donor with green nucleus and pink dotted cytoplasm is mated with recipient with black nucleus and blue diagonals cytoplasm. Upon cell fusion the cytoplasms mix, but often nuclei fail to fuse because of the presence of the *kar1* mutation that inhibits karyogamy. Selection is for cytoductants that bud off of the fused heterokaryon, which contain just the recipient's nucleus but a fusion of the donor and recipient cytoplasms.

(B) *Data showing transmission of p53 prion via cytoduction.* Subclones of L3672 containing p53 prions as well as isogenic control L3671 lacking prions were used as cytoplasmic donors by crossing them to a recipient non-prion *kar1* strain, L3663, transformed with pGPD-p53-EYFP or pGPD-p53-R175H-EYFP. Cytoductants, with mixed cytoplasm but recipient nuclei, were assayed for cytoplasmic fluorescent foci. All those obtained from the non-prion donor showed >95% cells with only nuclear fluorescence, whereas 38/44 and 23/28 of the cytoductants obtained from the prion donor, respectively, into wild-type or R175H p53 recipients showed ~30%–40% cells with cytoplasmic fluorescent foci. The dramatic difference in the fraction of cells with foci (~30%–40% versus approximately <5%) seen in the cytoductants made it easy to score them as containing or lacking the prion, as there were no cytoductants with an intermediate level of foci. Scale bar, 5 μM. See also Tables S1 and S2 for a description of strains and plasmids.

examined EYFP fluorescence in cytoductants (Figure 2B). In 38 of 44 p53 wild-type cytoductants obtained with the prion donor, ~30% of the cells had cytoplasmic foci. In 23 of 28 p53 analogous mutant cytoductants cytoplasmic foci were observed in ~40% cells. For the wild-type p53 prion cytoductants there were frequently more than two cytoplasmic dots per cell and some were large and irregular in shape. For the mutant p53 prion cytoductants most cells with foci contained only one or two dots and these were small, round, and of high intensity. Furthermore, the frequency and appearance of foci in the wild-type or mutant cytoductants were unchanged after >100 generations. Cytoductants obtained with control non-prion donor to either wild-type or mutant p53 recipients contained only about 5% cells with fluorescent cytoplasmic dots. The ability to cytoduce traits indicates that they are not dependent upon nuclear genes and is therefore diagnostic for cytoplasmic prions (Liebman and Chernoff, 2012). Thus, the finding of successful cytoduction of stable p53-EYFP aggregates strongly supports the idea that they are prions. Furthermore, the data show that wild-type p53 prions can induce mutant p53-R175H proteins to form a prion as efficiently as it induces wild-type p53 to form a prion.

We next asked if all cells in the cytoductant cultures had the prion, even though foci were only detected in ~30% or ~40% of the prion-containing cells. To do this we obtained 20 subclones from both a p53 wild-type and an R175H mutant cytoductant with aggregates. We found that 19 of 20 wild-type and all 20 mutant subclones contained the prion. Subclones scored as containing a prion showed the same ~30% or ~40% of the progeny with foci seen in the original cytoductants. The presence of nuclear fluorescence and absence of cytoplasmic aggregates in 95% of progeny from one of the 20 wild-type subclones indicates that the prion

is occasionally lost, as has been seen for other prions in yeast (Liebman and Chernoff, 2012). In contrast, in control cytoductants without foci all the 20 wild-type and 18 of 20 mutant subclones had 95% of progeny with nuclear p53 fluorescence and no cytoplasmic foci. The remaining two mutant subclones contained only about 10% cells with foci, in agreement with our general observations that non-prion cells with the p53-R175H mutant contain more cytoplasmic foci than cells with wild-type p53. Taken together, the results show that most cells in the wild-type or mutant cytoductant cultures with foci contain the prion, even though we only see aggregates, respectively, in ∼30% and ∼40% of the wild-type and mutant cells.

Non-aggregated p53-EYFP in recipient cells becomes aggregated when transfected with lysates of strains with heritable p53 aggregates or with p53 amyloid-like protein peptide

Lysates of the isogenic strains with (L3672) and without (L3671) the p53 prion were co-transfected, along with plasmid p*GPD-p53-EYFP,* into recipients (L3628 or L3719) that that lacked p53 (Figure 3). Of 50 p*GPD-p53-EYFP* L3628 transformants with the control lysate, none contained more than 1% cells with cytoplasmic aggregates (Figure 3B). In contrast, 97 of 248 transfectants with prion lysate had more than 10% cells with cytoplasmic foci and without nuclear p53 fluorescence (Figures 3A and 3B).

Also, when p*GPD-p53-EYFP* and *in vitro*-made amyloid fibers of the p53 fragment P8 (aa 250–257) were co-transfected into the L3628 recipient, fluorescent aggregates were frequently present in the transformants: 24 of 50 transformants showed about >10% cells with p53-EYFP cytoplasmic foci (Figure 3B). Controls transformed with p*GPD-p53-EYFP* without P8 showed essentially only nuclear fluorescence without cytoplasmic foci. Thus, amyloid seed made of a p53 peptide is sufficient to induce *in vivo* p53-EYFP aggregation. Induction of heritable p53-EYFP aggregation by transformation with a p53 peptide aggregate is strong evidence for protein-based prion inheritance.

To ask if the transfectants could maintain the p53 prion we propagated three transfectants of L3719 obtained from prion or non-prion lysates, and three obtained from P8 polymer or plasmid only, each for >100 generations. Both before and after the 100-generation propagation there were statistically significant increases in the percent of cells with foci in the transformants relative to control cultures p= <0.05 (Figure 3C). There was no statistical difference (p=>0.05) between the frequency of cells with foci in transformant cultures obtained from prion lysates whether they were examined soon after transformation or following 100 generations, but there was a reduction (p=<0.05) in the frequency of cells with foci in P8 transfectants after 100 generations. This is not surprising because unlike transfection with the lysates containing aggregates of a single heritable prion variant, transfection with the P8 polymer would be inducing the *de novo* formation of different types (variants) of prion-like aggregates, and these are often unstable (Liebman and Chernoff, 2012).

Transient interruption of p53 expression causes loss of the p53 prion

Transmission of a prion requires the continued presence of the prion seed. Thus, one test for a prion is to show that inhibiting expression of the prion protein, which causes loss of all prion seeds, prevents re-seeding of the prion protein when it is re-expressed (Wickner, 1994). To perform this test for the p53 prion we cultured the prion containing isolate L3672 and its isogenic non-prion control L3671, both carrying pADH-p53 (*LEU2*) and pGAL-p53-EYFP (*TRP1*), on non-plasmid-selective glucose medium for many generations. We then plated for individual cells and obtained five colonies from L3672 that lost pADH-p53 (were Leu⁻) but retained pGAL-p53-EYFP (were Trp⁺). These cells did not express p53 when grown on glucose. When returned to galactose, they all failed to form fluorescent foci, indicating p53-EYFP was not seeded to form a prion (Figure 4A). Furthermore, as seen in Figure 4B, their (rows 7 and 8) growth on galactose looked identical to isolates from the non-prion control strain that lost pADH-p53 (rows 3 and 4) and better than subclones that retain the prion (rows 5 and 6). Thus, as expected for a prion, transient interruption of p53 expression by losing the pADH-p53 plasmid in a prion strain and growing it on glucose where pGAL-p53-EYFP could not express p53-YFP, caused permanent loss of the prion when the cells were returned to galactose where p53-EYFP was expressed.

P53 forms reversible cytoplasmic foci that do not stain with ThT in response to various stresses

When yIG397 transformed with pGPD-p53-EYFP was grown on plasmid-selective glucose media, cells showed largely nuclear diffuse fluorescence (Figures 5A left and S1). However, 30 min after transfer of the cells to medium with 2% ethanol instead of glucose, cytoplasmic fluorescent foci appeared. Nuclear
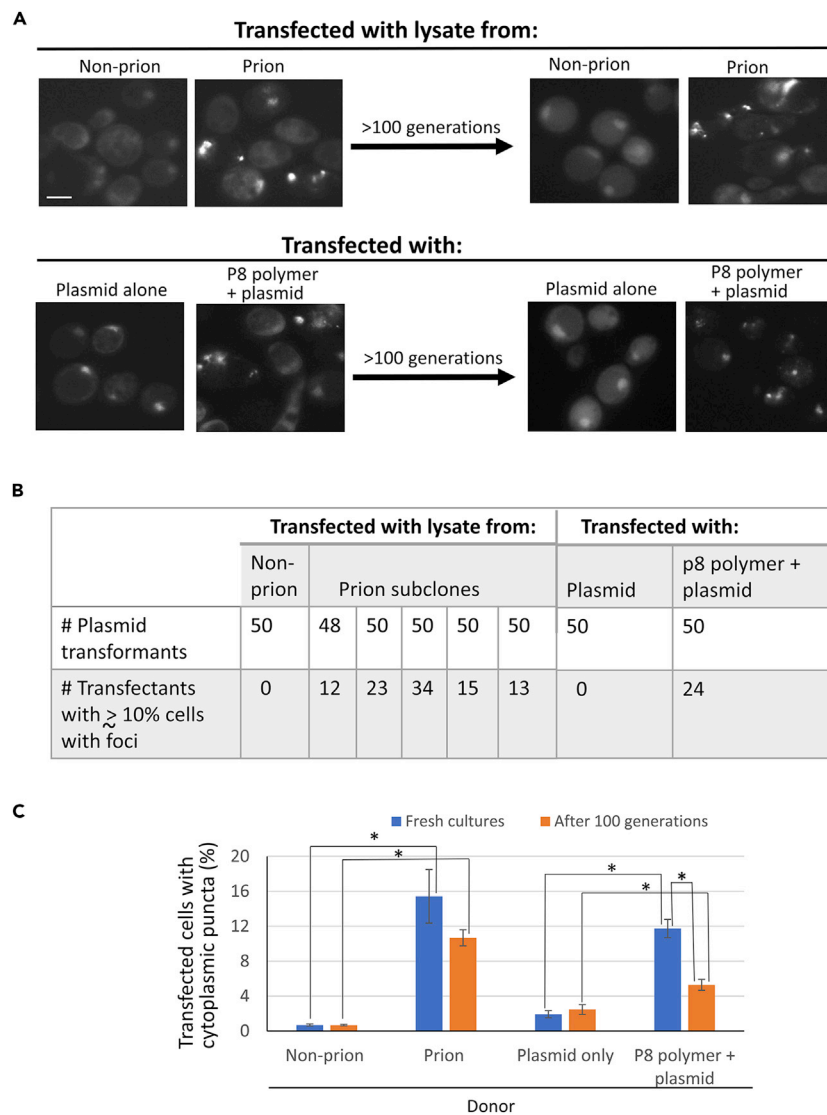
Figure 3. p53 prion-like aggregates can be transferred by transfection

(A) *Cell lysate from p53 prion yeast, or in vitro-made P8 polymer, promote the appearance of p53 cytoplasmic foci in transfectants.* Cleared cell lysates of p53 prion (L3672) or control non-prion cells (L3671) or P8 polymer of the p53 peptide or empty control were co-transformed with pGPD-p53-EYFP into *ADE2* p53 reporter strains L3628 or L3719 lacking p53. Successful transfection was scored by the appearance of cytoplasmic fluorescent foci. Retention of foci was scored after >100 generations. Scale bar, 5 μM.

(B) *The frequency of prion transfection is ∼ 25%–50%.* Shown are data for plasmid transformants into strain L3628, which were considered to be transfectants of prion lysates or P8 that seeded p53 aggregation if they had greater than or approximately 10% cells with cytoplasmic p53-EYFP foci. Plasmid transformants scored as not being transfected looked like controls with minimal foci.

(C) *Frequency of cells with foci in transfectants and transformation controls.* Each bar represents counts of 150–300 cells for each of the three L3719 transfectants or controls. Standard error is shown. Blue bars are data from initial transfectants or controls. Orange bars are data from their subclones after >100 generations. *p=<0.05.

foci were also sometimes seen following stress (Figure 5A) but were hard to score and distinguish from unstressed nuclei. We counted foci in the cytoplasm of about 25% of cells (Figure 5A middle), and the formation of these foci was independent of the HSP104 chaperone (Figure S2D). These foci remained as long as the cells were retained on ethanol medium. However, after 30 min of return to glucose medium both the nuclear and cytoplasmic foci disappeared (Figure 5A right). Similar results were obtained when cells were stressed with heat or glucose starvation (Figure 5A). These stress-induced p53 foci are reminiscent
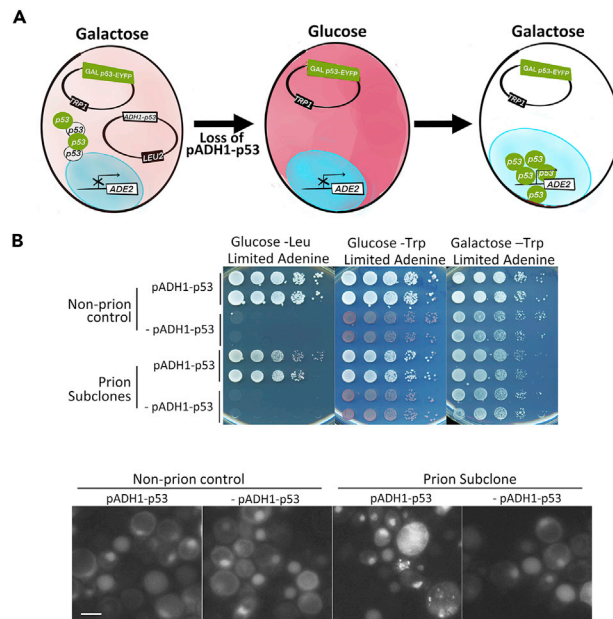
Figure 4. Transient loss of p53 cures cells of p53 prion

(A) *Cartoon showing how transient loss of p53 cures cells of the prion.* A prion containing cell, grown on galactose, is shown on the left. After loss of the ADH1-p53 plasmid this strain is grown on glucose, where no p53 is expressed (middle). Then upon return to galactose (right) there is no remaining prion seed, so the newly made tagged p53 remains diffuse in the nucleus and is able to turn on expression of the *ADE2* reporter.

(B) Data showing that transient absence of p53 causes permanent loss of the p53 prion. Prion strain L3672, and its isogenic non-prion control L3671, both carrying pADH-p53 (*LEU2*) and pGAL-p53-EYFP (*TRP1*), were grown on non-plasmid-selective glucose medium for many generations to allow for loss of the pADH-p53 plasmid. Cells that were Leu⁻ indicating loss of pADH-p53 (-pADH-p53) but Trp⁺ indicating retention of pGAL-p53-EYFP were grown and spotted along with independent controls that retained pADH-p53 (pADH-p53) from cells with and without the prion (upper). Only pADH-p53, but not -pADH-p53, cells express any p53 when grown on glucose. When returned to galactose the -pADH-p53 isolates from the prion culture looked identical to non-prion control -pADH-p53, growing better on galactose medium with limiting adenine than prion pADH-53 controls that retained the prion. Two representative isolates of each type are shown. Furthermore, all -pADH-p53 isolates from the prion cells failed to form cytoplasmic fluorescent foci when grown on galactose, indicating that no p53 prion was present (bottom). Scale bar, 5 μM.

See also Tables S1 and S2 for a description of strains and plasmids.

of unstable liquid-like droplets formed by liquid-liquid phase separation of a variety of proteins with intrinsically disordered regions often in response to stress.

As short exposure to the aliphatic alcohol 1,6-hexanediol has been shown to dissolve liquid-like droplets but not solid protein assemblies (Kroschwald et al., 2017) we examined the effect of 1,6-hexanediol on the cytoplasmic stress-induced p53-EYFP foci when compared with the stable prion p53-EYFP foci. A 5-min treatment with 1,6-hexanediol caused the disappearance of >90% of the stress-induced foci but had no effect on prion foci (Figure 5C). A short exposure was required because, similar to a previous report (Kroschwald et al., 2017), longer treatment with 1,6-hexanediol actually caused the appearance of cytoplasmic fluorescent foci in all cells with wild-type p53-EYFP (Figure S3). Another difference we found between the prion foci and the unstable stress-induced foci is that only the former stain with ThT (Figure 5B). This suggests that the prion foci, but not the stress foci, are amyloid-like. Also, we found that the stress foci had the high circularity level expected of a liquid droplet (Kroschwald et al., 2015) unlike the prion foci that were less circular (Figure 5D). Curiously, we found that the cancer hotspot structural mutation p53-R175H prevents formation of the stress foci (Figure 5A).

P53 stress-induced cytoplasmic foci co-localize with P-bodies

Strain yIG397 was co-transformed with pGPD-p53-EYFP to allow for detection of p53-EYFP stress foci and either pEdc3-mCH or pDcp2-RFP to allow for detection of P-bodies. The cells were subjected to ethanol,
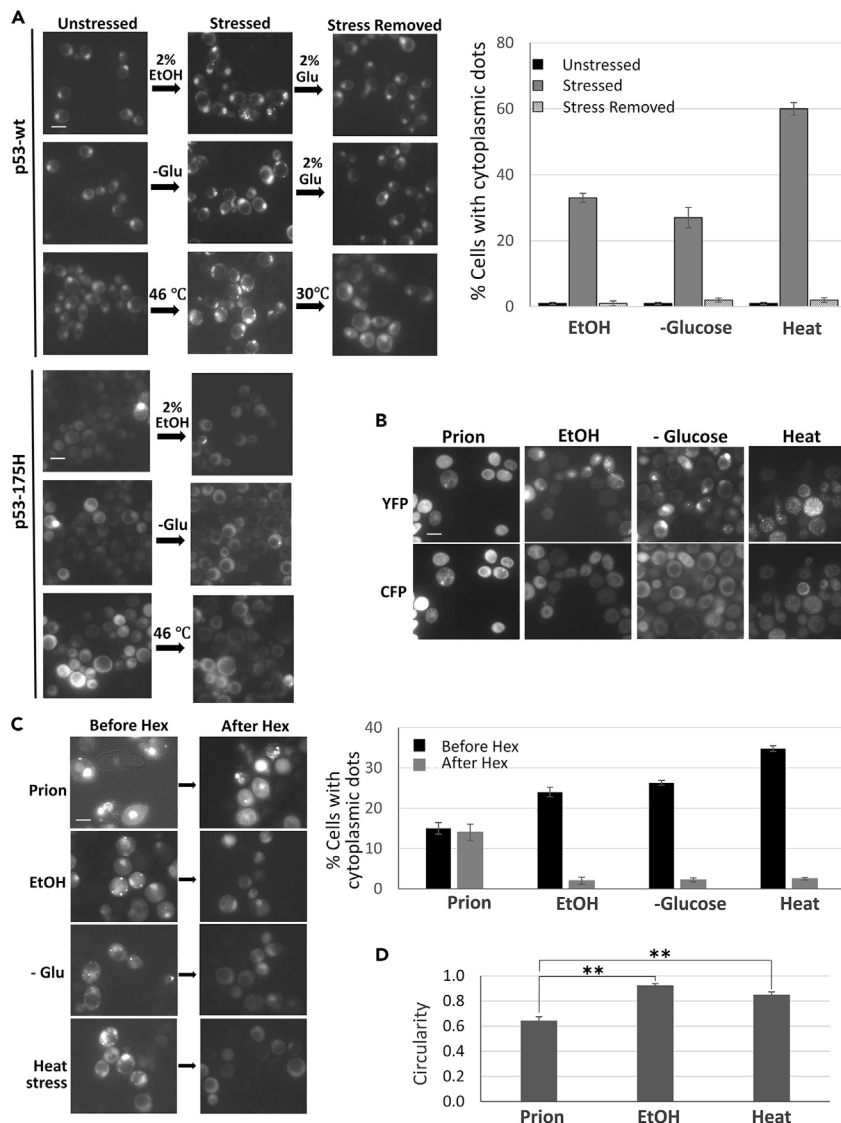
Figure 5. p53 can also form unstable foci

(A) *Ethanol, glucose starvation, and heat stress lead to the formation of p53 foci that disappear when the stress is removed.* Shown (three upper rows) is yIG397 transformed with pGPD-p53-EYFP grown on plasmid-selective glucose media (left), following stress: 30 min in medium with 2% ethanol, 30 min of glucose starvation or 10 min at 46°C (middle), and then after removal of stress (right). Graph shows the mean of counts from 3 independent transformants ± SEM. Three lower rows show yIG397 transformed with pGPD-p53-175H-EYFP under the same stresses. Arrowhead shows nucleus with foci on top of diffuse fluorescence. Scale bar, 5 μM.

(B) *Foci caused by stress do not stain with Thioflavin T.* Shown are cells with stress-induced p53-EYFP foci (obtained as in A above) or cells with prion p53-EYFP foci (obtained as in Figure 1E). Cells were fixed, stained with ThT, and examined for EYFP (YFP) fluorescence or ThT staining (CFP).

(C) *Hexanediol causes the disappearance of stress-induced, but not prion foci.* Shown are cells with stress-induced p53-EYFP foci (obtained as in A above) or cells with prion p53-EYFP foci (obtained as in Figure 1E) before (-Hex) and after (+Hex) 5-min treatments with 10% 1,6-hexanediol. Graph shows counts from three independent transformants ± SEM.

(D) *Circularity of stress versus prion foci.* Circularity of cytoplasmic aggregates in cells with stress or prion foci obtained as described in (C) (except 15 min of heat was given) was measured. ImageJ and the formula $(4 \ast \pi \ast area)/perimeter^2$ was used (n = 40 for each). A value of 1.0 indicates a perfect circular shape, and the lower the value, the less circular the aggregate. Shown are mean ± SEM. **p calculated with one-tailed t test as <0.005 is shown.

See also Figure S2 and Tables S1 and S2 for a description of strains and plasmids.

heat, or glucose starvation to induce the appearance of both EYFP-marked p53 foci and mCh- or RFP-marked P-bodies. These two types of foci were seen to partially co-localize (Figure 6).

DISCUSSION

In this work we show that wild-type p53 expressed in living yeast not only has the ability to propagate as a true prion accompanied by the appearance of stable cytoplasmic foci and reduction in p53 activity but also can also form unstable foci in response to stress. Inactivation of p53 via prion formation has a direct implication for the onset of cancer. Whether the unstable stress-induced foci affect the appearance of p53 prions remains to be determined.

Previous evidence suggested that p53 aggregates in some cancer cells (Ano Bom et al., 2012; De Smet et al., 2017; Gitler and Lehmann, 2012; Levy et al., 2011; Xu et al., 2011). Often p53 amyloid is found in nuclei of tumor cells as oligomers, leading to the suggestion that amyloid p53 oligomers in the nucleus could result in an oncogenic gain of function (Pedrote et al., 2020). Possibly fibrillar p53 would be present in the cytoplasm. One clear example of cytoplasmic p53 is the accumulation of amyloid Δ40p53 in endometrial carcinoma cells (Melo Dos Santos et al., 2019). Our data show that in yeast p53 can form stable, ThT stainable, cytoplasmic aggregates. Although foci are sometimes seen in nuclei, we have never observed nuclear staining with ThT. Why we observe largely cytoplasmic amyloid p53 in yeast rather than the nuclear p53 amyloid seen in tumor cells is unknown. As RNA is known to inhibit p53 foci formation (Kovachev et al., 2017) possibly the excess RNA in yeast nuclei inhibits p53 from forming amyloid.

The p53 cytoplasmic aggregates that we observe in yeast have the characteristics of prions: they not only self-seed but also continually replicate the seeds, causing the prion to be stable for over 100 generations. Also, we show that the prion causes loss of p53 function. Our finding that overexpression of p53 triggers it to form a heritable prion in yeast with reduced transcriptional activity suggests that increased levels of p53 may likewise trigger prion formation and concomitant p53 inactivation in animal cells, leading to cancer. Indeed high levels of p53 are often found in tumor cells (Houben et al., 2011), and stresses such as DNA damage that induce cancer often lead to an increase in the cellular level of p53 (Lavin and Gueven, 2006).

In addition, the ability of p53 to form a prion upends the classic idea that overexpression of wild-type p53 via gene therapy could cure cancers caused by p53-inactivating mutations. Such a treatment would not be expected to help if the inactivating mutations result in prion seeds that attract and therefore inactivate wild-type p53. Also, overexpression of wild-type p53 could generate prion seeds de novo that, instead of providing p53 activity, cause aggregation of the p53 mutant protein causing increased loss of activity. p53 prion protein could also trap and inactivate its related transcription factors, p63 and p73 (Billant et al., 2017), which could increase cancer pathology. In contrast, prion-like aggregates that do not multiply would have a more limited capacity to inactivate WT p53, p63, or p73.

Overexpression of p53 allowed us to isolate a strain of yeast that had cytoplasmic p53 aggregates and reduced p53 activity. These aggregates appear to be prions because they stained with ThT, suggestive of amyloid, and were stable for over 100 generations. Following centrifugation of cell lysates, the p53 aggregates were found in pellet fractions as seen for other prions. Also, like other prions, the cytoplasm of the p53 prion strain infected recipient cells with the prion via cytoduction. Also, the p53 prion was transferred to recipients by transfecting them with lysates from prion cells or with amyloid fibers of a p53-derived peptide (P8) made in vitro.

The question of how p53, when aggregated or non-aggregated, affects yeast growth is complicated and remains unresolved. As reported by others (Bischoff et al., 1992; Inga and Resnick, 2001; Kumar et al., 2017; Nigro et al., 1992), we have seen growth inhibition associated with overexpression of wild-type non-aggregated but not mutant p53 in some strain backgrounds. Assuming the inhibition is caused by excess p53 transcription factor activity, one would expect that the reduced activity associated with prion formation would rescue cells from the growth inhibition. Indeed, this hypothesis is supported by our finding that following transient overexpression of p53, pink colonies with inactive p53 and p53-EYFP aggregates pop out on a background of cells with active p53 following weeks of room-temperature incubation. However, even though there is no increase in dead cells among prion subclones (Figure 1E), in spot tests the prion causes a reduced growth rate even in the presence of adenine (Figure 1C). It is likely that p53 is largely non-functional and lacks toxic p53 amyloid in the subset of cells in the prion culture that have essentially only vacuolar fluorescence. These cells may grow better than cells in the prion culture with cytoplasmic dots
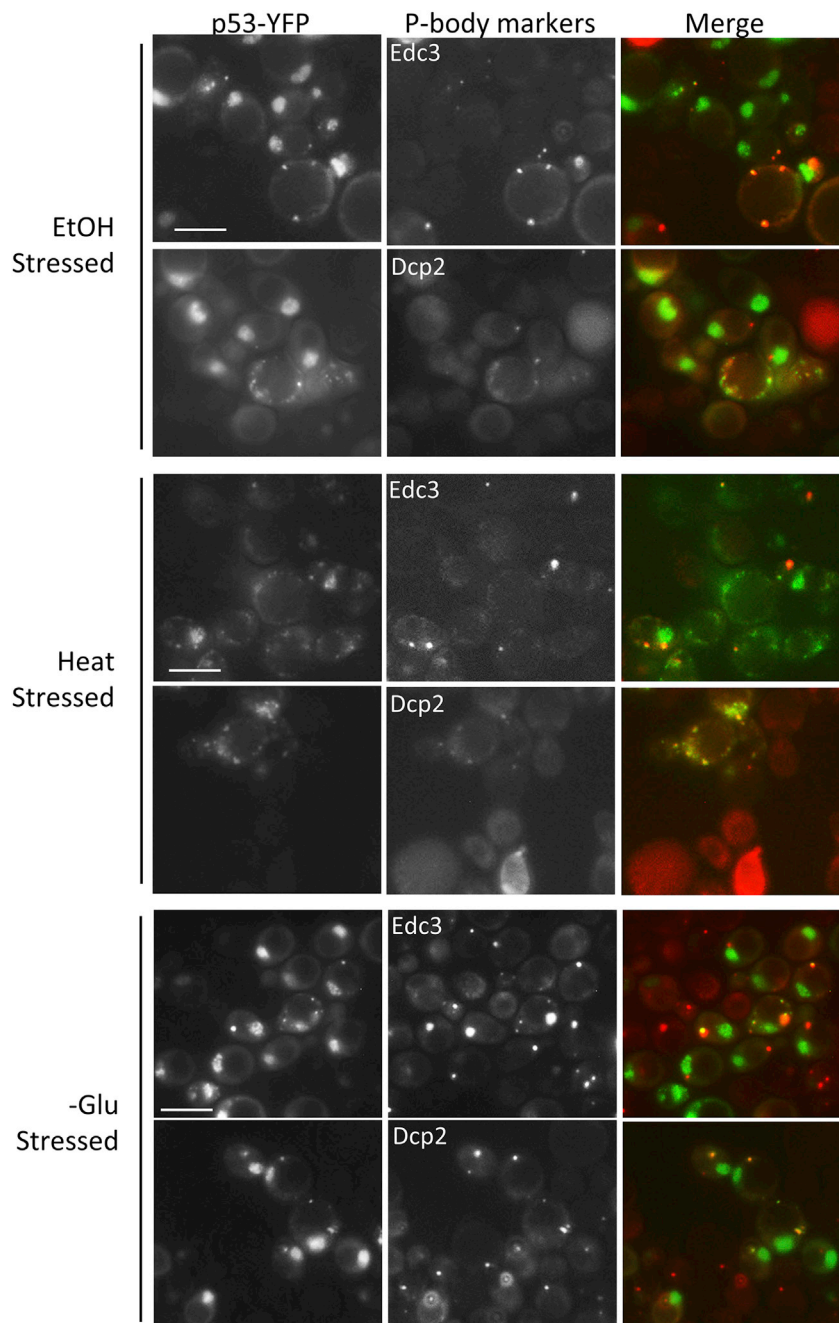
Figure 6. p53 stress foci co-localize with cellular P-bodies

Strain yIG397 was co-transformed with pGPD-p53-EYFP to allow for detection of p53-EYFP stress foci and either pEdc3-mCH or pDcp2-RFP to allow for detection of P-bodies. The cells were subjected to ethanol, heat, or glucose starvation to induce the appearance of both EYFP-marked p53 foci and mCh- or RFP-marked P-bodies and were photographed, respectively, with YFP and mCh filters. Scale bar, 5 μM.

See also Tables S1 and S2 for a description of strains and plasmids.

because they lack significant toxic amyloid aggregates. They also may grow better than prion or non-prion cells with nuclear fluorescence because of their reduced level of nuclear p53 and therefore reduced toxicity associated with excess nuclear p53 (Bischoff et al., 1992; Inga and Resnick, 2001; Kumar et al., 2017; Nigro et al., 1992). These cells could arise if p53 prion intermediate structures were directed to the vacuole for degradation before a stable prion was formed.

Whether wild-type p53 aggregates seed aggregation of heterologous proteins can now be determined. We show that one cancer-causing p53 mutant, p53-R175H, is seeded to form a prion by the wild-type p53 prion. Whether other p53 mutants are able to form prions can now be established. It should also be possible to use yeast to select for p53 mutants that cannot join prion aggregates but retain transcription factor activity. If such mutants were used in gene therapy, they would avoid the prion associated problems described above and could provide a useful therapy for cancer. Also, our results have the potential to be used for high-throughput screening of compounds with potential antitumoral activity for drugs that target aggregation of p53. This would complement recent targeted approaches for such drugs (Rangel et al., 2019; Silva et al., 2018; Soragni et al., 2016).

Interestingly, non-membrane-bound foci of a variety of proteins, including P-bodies, have been described that appear to arise from LLPS. p53 has also been shown to be present in such non membrane-bound liquid-like nuclear droplets, including Cajal and promyelocytic leukemia protein bodies (Banani et al., 2017; Cioce and Lamond, 2005; Fogal et al., 2000; Guo et al., 2000). p53 can also form liquid-like droplets *in vitro* (Kamagata et al., 2020). Now we show that p53 can form unstable foci in live yeast in response to ethanol, heat, and glucose starvation. These stresses also induce the appearance of P-bodies previously shown to be liquid droplets in yeast (Kroschwald et al., 2015), and we show that some p53 stress foci co-localize with the P-bodies. Like P-bodies, the p53 stress foci are distinct from amyloid-like stable foci because they disappear rapidly when the stresses are removed, do not stain with ThT, and are dissolved by 1,6-hexanediol. The foci located in the cytoplasm are unlikely to promote transcription, but the effect of the nuclear stress foci on transcription is unknown.

Increasingly LLPS, or related structures (McSwiggen et al., 2019), have been found to affect transcription. Enhanced or reduced activity of transcription factors has been seen when they join LLPS foci (Cho et al., 2018; Chong et al., 2018; Sabari et al., 2018; Tarczewska and Greb-Markiewicz, 2019). Our demonstration that the transcription factor p53 forms unstable foci in yeast in response to stress opens the possibility that p53 activity is likewise regulated by phase transition. Possibly stresses that promote the formation of the foci enhance or reduce the activity of p53, leading to important cellular ramifications. Indeed, we have shown that mutations in p53 can prevent it from forming stress foci: the p53-175H mutation associated with cancer that inactivates p53 fails to form stress foci.

Limitations of the study
This work used an yeast model to show that p53 can form a stable prion as well as liquid-like droplets. Although yeast is a eukaryote and has proved to be a useful model for mammalian diseases, there are many differences between yeast and mammalian cells, differences in chaperones.

Resource availability
Lead contact
Susan W. Liebman sliebman@unr.edu can be contacted for all strains and plasmids used.

Materials availability
All unique/stable reagents generated in this study are available from the Lead Contact without restriction.

Data and code availability
This study did not generate the datasets.

METHODS
All methods can be found in the accompanying Transparent Methods supplemental file.

SUPPLEMENTAL INFORMATION
Supplemental information can be found online at https://doi.org/10.1016/j.isci.2020.102000.

AUTHOR CONTRIBUTIONS

S.-K.P., S.P., and C.P. conducted experiments. S.-K.P. and S.W.L. designed experiments. S.-K.P., S.P., and S.W.L. prepared the figures and edited the paper. S.W.L. wrote the paper.

DECLARATION OF INTERESTS

The authors declare no competing interests.

REFERENCES

Alberti, S., Halfmann, R., King, O., Kapila, A., and Lindquist, S. (2009). A systematic survey identifies prions and illuminates sequence features of prionogenic proteins. Cell 137, 146–158.

Ano Bom, A.P., Rangel, L.P., Costa, D.C., de Oliveira, G.A., Sanches, D., Braga, C.A., Gava, L.M., Ramos, C.H., Cepeda, A.O., Stumbo, A.C., et al. (2012). Mutant p53 aggregates into prion-like amyloid oligomers and fibrils: implications for cancer. J. Biol. Chem. 287, 28152–28162.

Armakola, M., Hart, M.P., and Gitler, A.D. (2011). TDP-43 toxicity in yeast. Methods 53, 238–245.

Arslan, F., Hong, J.Y., Kanneganti, V., Park, S.K., and Liebman, S.W. (2015). Heterologous aggregates promote de novo prion appearance via more than one mechanism. PLoS Genet. 11, e1004814.

Bagriantsev, S., and Liebman, S. (2006). Modulation of Abeta42 low-n oligomerization using a novel yeast reporter system. BMC Biol. 4, 32.

Banani, S.F., Lee, H.O., Hyman, A.A., and Rosen, M.K. (2017). Biomolecular condensates: organizers of cellular biochemistry. Nat. Rev. Mol. Cell Biol. 18, 285–298.

Billant, O., Blondel, M., and Voisset, C. (2017). p53, p63 and p73 in the wonderland of S. cerevisiae. Oncotarget 8, 57855–57869.

Bischoff, J.R., Casso, D., and Beach, D. (1992). Human p53 inhibits growth in Schizosaccharomyces pombe. Mol. Cell. Biol. 12, 1405–1411.

Boeynaems, S., Alberti, S., Fawzi, N.L., Mittag, T., Polymenidou, M., Rousseau, F., Schymkowitz, J., Shorter, J., Wolozin, B., Van Den Bosch, L., et al. (2018). Protein phase separation: a new phase in cell biology. Trends Cell Biol. 28, 420–435.

Boncella, A.E., Shattuck, J.E., Cascarina, S.M., Paul, K.R., Baer, M.H., Fomicheva, A., Lamb, A.K., and Ross, E.D. (2020). Composition-based prediction and rational manipulation of prion-like domain recruitment to stress granules. Proc. Natl. Acad. Sci. U S A 117, 5826–5835.

Bonini, N.M., and Gitler, A.D. (2011). Model organisms reveal insight into human neurodegenerative disease: ataxin-2 intermediate-length polyglutamine expansions are a risk factor for ALS. J. Mol. Neurosci. 45, 676–683.

Buchan, J.R., Yoon, J.H., and Parker, R. (2011). Stress-specific composition, assembly and kinetics of stress granules in Saccharomyces cerevisiae. J. Cell Sci. 124, 228–239.

Byers, J.S., and Jarosz, D.F. (2017). High-throughput screening for protein-based inheritance in S. cerevisiae. J. Vis. Exp. 8, 56069.

Caudron, F., and Barral, Y. (2013). A super-assembly of Whi3 encodes memory of deceptive encounters by single cells during yeast courtship. Cell 155, 1244–1257.

Chakrabortee, S., Byers, J.S., Jones, S., Garcia, D.M., Bhullar, B., Chang, A., She, R., Lee, L., Fremin, B., Lindquist, S., et al. (2016). Intrinsically disordered proteins drive emergence and inheritance of biological traits. Cell 167, 369–381 e312.

Chakravarty, A.K., and Jarosz, D.F. (2018). More than just a phase: prions at the crossroads of epigenetic inheritance and evolutionary change. J. Mol. Biol. 430, 4607–4618.

Chakravarty, A.K., Smejkal, T., Itakura, A.K., Garcia, D.M., and Jarosz, D.F. (2020). A non-amyloid prion particle that activates a heritable gene expression program. Mol. Cell 77, 251–265 e259.

Chernoff, Y.O., Lindquist, S.L., Ono, B., Inge-Vechtomov, S.G., and Liebman, S.W. (1995). Role of the chaperone protein Hsp104 in propagation of the yeast prion-like factor [psi+]. Science 268, 880–884.

Chiti, F., and Dobson, C.M. (2006). Protein misfolding, functional amyloid, and human disease. Annu. Rev. Biochem. 75, 333–366.

Cho, W.K., Spille, J.H., Hecht, M., Lee, C., Li, C., Grube, V., and Cisse, , II. (2018). Mediator and RNA polymerase II clusters associate in transcription-dependent condensates. Science 361, 412–415.

Chong, S., Dugast-Darzacq, C., Liu, Z., Dong, P., Dailey, G.M., Cattoglio, C., Heckert, A., Banala, S., Lavis, L., Darzacq, X., et al. (2018). Imaging dynamic and selective low-complexity domain interactions that control gene transcription. Science 361, eaar2555.

Cioce, M., and Lamond, A.I. (2005). Cajal bodies: a long history of discovery. Annu. Rev. Cell Dev. Biol. 21, 105–131.

Conde, J., and Fink, G.R. (1976). A mutant of Saccharomyces cerevisiae defective for nuclear fusion. Proc. Natl. Acad. Sci. U S A 73, 3651–3655.

de Oliveira, G.A.P., Petronilho, E.C., Pedrote, M.M., Marques, M.A., Vieira, T., Cino, E.A., and Silva, J.L. (2020). The status of p53 oligomeric and aggregation states in cancer. Biomolecules 10, 548.

De Smet, F., Saiz Rubio, M., Hompes, D., Naus, E., De Baets, G., Langenberg, T., Hipp, M.S., Houben, B., Claes, F., Charbonneau, S., et al. (2017). Nuclear inclusion bodies of mutant and wild-type p53 in cancer: a hallmark of p53 inactivation and proteostasis remodelling by p53 aggregation. J. Pathol. 242, 24–38.

Derkatch, I.L., Chernoff, Y.O., Kushnirov, V.V., Inge-Vechtomov, S.G., and Liebman, S.W. (1996). Genesis and variability of [PSI] prion factors in Saccharomyces cerevisiae. Genetics 144, 1375–1386.

Du, Z., Park, K.W., Yu, H., Fan, Q., and Li, L. (2008). Newly identified prion linked to the chromatin-remodeling factor Swi1 in Saccharomyces cerevisiae. Nat. Genet. 40, 460–465.

Elledge, R.M., Clark, G.M., Fuqua, S.A., Yu, Y.Y., and Allred, D.C. (1994). p53 protein accumulation detected by five different antibodies: relationship to prognosis and heat shock protein 70 in breast cancer. Cancer Res. 54, 3752–3757.

Fogal, V., Gostissa, M., Sandy, P., Zacchi, P., Sternsdorf, T., Jensen, K., Pandolfi, P.P., Will, H., Schneider, C., and Del Sal, G. (2000). Regulation

of p53 activity in nuclear bodies by a specific PML isoform. EMBO J. 19, 6185–6195.

Fronza, G., Inga, A., Monti, P., Scott, G., Campomenosi, P., Menichini, P., Ottaggio, L., Viaggi, S., Burns, P.A., Gold, B., et al. (2000). The yeast p53 functional assay: a new tool for molecular epidemiology. Hopes and facts. Mutat. Res. 462, 293–301.

Ghosh, S., Ghosh, D., Ranganathan, S., Anoop, A., P, S.K., Jha, N.N., Padinhateeri, R., and Maji, S.K. (2014). Investigating the intrinsic aggregation potential of evolutionarily conserved segments in p53. Biochemistry 53, 5995–6010.

Ghosh, S., Salot, S., Sengupta, S., Navalkar, A., Ghosh, D., Jacob, R., Das, S., Kumar, R., Jha, N.N., Sahay, S., et al. (2017). p53 amyloid formation leading to its loss of function: implications in cancer pathogenesis. Cell Death Differ. 24, 1784–1798.

Gitler, A.D., and Lehmann, R. (2012). Modeling human disease. Science 337, 269.

Grousl, T., Ivanov, P., Malcova, I., Pompach, P., Frydlova, I., Slaba, R., Senohrabkova, L., Novakova, L., and Hasek, J. (2013). Heat shock-induced accumulation of translation elongation and termination factors precedes assembly of stress granules in S. cerevisiae. PloS one 8, e57083.

Guo, A., Salomoni, P., Luo, J., Shih, A., Zhong, S., Gu, W., and Pandolfi, P.P. (2000). The function of PML in p53-dependent apoptosis. Nat. Cell Biol. 2, 730–736.

Harvey, Z.H., Chakravarty, A.K., Futia, R.A., and Jarosz, D.F. (2020). A prion epigenetic switch establishes an active chromatin state. Cell 180, 928–940 e914.

Houben, R., Hesbacher, S., Schmid, C.P., Kauczok, C.S., Flohr, U., Haferkamp, S., Muller, C.S., Schrama, D., Wischhusen, J., and Becker, J.C. (2011). High-level expression of wild-type p53 in melanoma cells is frequently associated with inactivity in p53 reporter gene assays. PloS one 6, e22096.

Inga, A., Cresta, S., Monti, P., Aprile, A., Scott, G., Abbondandolo, A., Iggo, R., and Fronza, G. (1997). Simple identification of dominant p53 mutants by a yeast functional assay. Carcinogenesis 18, 2019–2021.

Inga, A., and Resnick, M.A. (2001). Novel human p53 mutations that are toxic to yeast can enhance transactivation of specific promoters and reactivate tumor p53 mutants. Oncogene 20, 3409–3419.

Itakura, A.K., Chakravarty, A.K., Jakobson, C.M., and Jarosz, D.F. (2020). Widespread prion-based control of growth and differentiation strategies in Saccharomyces cerevisiae. Mol. Cell 77, 266–278 e266.

Itakura, A.K., Futia, R.A., and Jarosz, D.F. (2018). It pays to Be in phase. Biochemistry 57, 2520–2529.

Iwakuma, T., Lozano, G., and Flores, E.R. (2005). Li-Fraumeni syndrome: a p53 family affair. Cell Cycle 4, 865–867.

Jin, M., Fuller, G.G., Han, T., Yao, Y., Alessi, A.F., Freeberg, M.A., Roach, N.P., Moresco, J.J.,

Karnovsky, A., Baba, M., et al. (2017). Glycolytic enzymes coalesce in G bodies under hypoxic stress. Cell Rep. 20, 895–908.

Kamagata, K., Kanbayashi, S., Honda, M., Itoh, Y., Takahashi, H., Kameda, T., Nagatsugi, F., and Takahashi, S. (2020). Liquid-like droplet formation by tumor suppressor p53 induced by multivalent electrostatic interactions between two disordered domains. Sci. Rep. 10, 580.

King, C.Y., and Diaz-Avalos, R. (2004). Protein-only transmission of three yeast prion strains. Nature 428, 319–323.

Kovachev, P.S., Banerjee, D., Rangel, L.P., Eriksson, J., Pedrote, M.M., Martins-Dinis, M., Edwards, K., Cordeiro, Y., Silva, J.L., and Sanyal, S. (2017). Distinct modulatory role of RNA in the aggregation of the tumor suppressor protein p53 core domain. J. Biol. Chem. 292, 9345–9357.

Kroschwald, S., Maharana, S., Mateju, D., Malinovska, L., Nuske, E., Poser, I., Richter, D., and Alberti, S. (2015). Promiscuous interactions and protein disaggregases determine the material state of stress-inducible RNP granules. Elife 4, e06807.

Kroschwald, S., Shovamayee, M., and Alberti, S. (2017). Hexanediol: a chemical probe to investigate the material properties of membrane-less compartments. Matters 3, e201702000010.

Kumar, A., Dandekar, J.U., and Bhat, P.J. (2017). Fermentative metabolism impedes p53-dependent apoptosis in a Crabtree-positive but not in Crabtree-negative yeast. J. Biosci. 42, 585–601.

Lane, D.P. (1992). Cancer. p53, guardian of the genome. Nature 358, 15–16.

Lavin, M.F., and Gueven, N. (2006). The complexity of p53 stabilization and activation. Cell Death Differ. 13, 941–950.

Lee, H.Y., Chao, J.C., Cheng, K.Y., and Leu, J.Y. (2018). Misfolding-prone proteins are reversibly sequestered to an Hsp42-associated granule upon chronological aging. J. Cell Sci. 131, jcs220202.

Levine, A.J., and Oren, M. (2009). The first 30 years of p53: growing ever more complex. Nat. Rev. Cancer 9, 749–758.

Levine, A.J., Tomasini, R., McKeon, F.D., Mak, T.W., and Melino, G. (2011). The p53 family: guardians of maternal reproduction. Nat. Rev. Mol. Cell Biol. 12, 259–265.

Levy, C.B., Stumbo, A.C., Ano Bom, A.P., Portari, E.A., Cordeiro, Y., Silva, J.L., and De Moura-Gallo, C.V. (2011). Co-localization of mutant p53 and amyloid-like protein aggregates in breast tumors. Int. J. Biochem. Cell Biol. 43, 60–64.

Liebman, S.W., and Chernoff, Y.O. (2012). Prions in yeast. Genetics 191, 1041–1072.

March, Z.M., King, O.D., and Shorter, J. (2016). Prion-like domains as epigenetic regulators, scaffolds for subcellular organization, and drivers of neurodegenerative disease. Brain Res. 1647, 9–18.

Marchante, R., Beal, D.M., Koloteva-Levine, N., Purton, T.J., Tuite, M.F., and Xue, W.F. (2017). The

physical dimensions of amyloid aggregates control their infective potential as prion particles. Elife 6, e27109.

McSwiggen, D.T., Mir, M., Darzacq, X., and Tjian, R. (2019). Evaluating phase separation in live cells: diagnosis, caveats, and functional consequences. Genes Dev. 33, 1619–1634.

Melo Dos Santos, N., de Oliveira, G.A.P., Ramos Rocha, M., Pedrote, M.M., Diniz da Silva Ferretti, G., Pereira Rangel, L., Morgado-Diaz, J.A., Silva, J.L., and Rodrigues Pereira Gimba, E. (2019). Loss of the p53 transactivation domain results in high amyloid aggregation of the Delta40p53 isoform in endometrial carcinoma cells. J. Biol. Chem. 294, 9430–9439.

Moll, U.M., LaQuaglia, M., Benard, J., and Riou, G. (1995). Wild-type p53 protein undergoes cytoplasmic sequestration in undifferentiated neuroblastomas but not in differentiated tumors. Proc. Natl. Acad. Sci. U S A 92, 4407–4411.

Moll, U.M., Valea, F., and Chumas, J. (1997). Role of p53 alteration in primary peritoneal carcinoma. Int. J. Gynecol. Pathol. 16, 156–162.

Monti, P., Bosco, B., Gomes, S., Saraiva, L., Fronza, G., and Inga, A. (2019). Yeast as a chassis for developing functional assays to study human P53. J. Vis. Exp. https://doi.org/10.3791/59071.

Narayanaswamy, R., Levy, M., Tschansky, M., Stovall, G.M., O'Connell, J.D., Mirrielees, J., Ellington, A.D., and Marcotte, E.M. (2009). Widespread reorganization of metabolic enzymes into reversible assemblies upon nutrient starvation. Proc. Natl. Acad. Sci. U S A 106, 10147–10152.

Navalkar, A., Ghosh, S., Pandey, S., Paul, A., Datta, D., and Maji, S.K. (2020). Prion-like p53 amyloids in cancer. Biochemistry 59, 146–155.

Nigro, J.M., Sikorski, R., Reed, S.I., and Vogelstein, B. (1992). Human p53 and CDC2Hs genes combine to inhibit the proliferation of Saccharomyces cerevisiae. Mol. Cell. Biol. 12, 1357–1365.

Osherovich, L.Z., Cox, B.S., Tuite, M.F., and Weissman, J.S. (2004). Dissection and design of yeast prions. PLoS Biol. 2, E86.

Ozaki, T., and Nakagawara, A. (2011). p53: the attractive tumor suppressor in the cancer research field. J. Biomed. Biotechnol. 2011, 603925.

Park, S., Park, S.K., Watanabe, N., Hashimoto, T., Iwatsubo, T., Shelkovnikova, T.A., and Liebman, S.W. (2019). Calcium-responsive transactivator (CREST) toxicity is rescued by loss of PBP1/ATXN2 function in a novel yeast proteinopathy model and in transgenic flies. PLoS Genet. 15, e1008308.

Park, S.K., Hong, J.Y., Arslan, F., Kanneganti, V., Patel, B., Tietsort, A., Tank, E.M.H., Li, X., Barmada, S.J., and Liebman, S.W. (2017). Overexpression of the essential Sis1 chaperone reduces TDP-43 effects on toxicity and proteolysis. PLoS Genet. 13, e1006805.

Park, S.K., Pegan, S.D., Mesecar, A.D., Jungbauer, L.M., LaDu, M.J., and Liebman, S.W. (2011). Development and validation of a yeast high-throughput screen for inhibitors of

Abeta(4)(2) oligomerization. Dis. Models Mech. *4*, 822–831.

Patel, B.K., Gavin-Smyth, J., and Liebman, S.W. (2009). The yeast global transcriptional co-repressor protein Cyc8 can propagate as a prion. Nat. Cell Biol. *11*, 344–349.

Pedrote, M.M., Motta, M.F., Ferretti, G.D.S., Norberto, D.R., Spohr, T., Lima, F.R.S., Gratton, E., Silva, J.L., and de Oliveira, G.A.P. (2020). Oncogenic gain of function in glioblastoma is linked to mutant p53 amyloid oligomers. iScience *23*, 100820.

Pezza, J.A., Villali, J., Sindi, S.S., and Serio, T.R. (2014). Amyloid-associated activity contributes to the severity and toxicity of a prion phenotype. Nat. Commun. *5*, 4384.

Rangel, L.P., Ferretti, G.D.S., Costa, C.L., Andrade, S., Carvalho, R.S., Costa, D.C.F., and Silva, J.L. (2019). p53 reactivation with induction of massive apoptosis-1 (PRIMA-1) inhibits amyloid aggregation of mutant p53 in cancer cells. J. Biol. Chem. *294*, 3670–3682.

Sabari, B.R., Dall'Agnese, A., Boija, A., Klein, I.A., Coffey, E.L., Shrinivas, K., Abraham, B.J., Hannett, N.M., Zamudio, A.V., Manteiga, J.C., et al. (2018). Coactivator condensation at super-enhancers

links phase separation and gene control. Science *361*, eaar3958.

Sharma, S.V., Agatsuma, T., and Nakano, H. (1998). Targeting of the protein chaperone, HSP90, by the transformation suppressing agent, radicicol. Oncogene *16*, 2639–2645.

Silva, J.L., Cino, E.A., Soares, I.N., Ferreira, V.F., and G, A.P.d.O. (2018). Targeting the prion-like aggregation of mutant p53 to combat cancer. Acc. Chem. Res. *51*, 181–190.

Soragni, A., Janzen, D.M., Johnson, L.M., Lindgren, A.G., Thai-Quynh Nguyen, A., Tiourin, E., Soriaga, A.B., Lu, J., Jiang, L., Faull, K.F., et al. (2016). A designed inhibitor of p53 aggregation rescues p53 tumor suppression in ovarian carcinomas. Cancer Cell *29*, 90–103.

Summers, D.W., and Cyr, D.M. (2011). Use of yeast as a system to study amyloid toxicity. Methods *53*, 226–231.

Tanaka, M., Chien, P., Naber, N., Cooke, R., and Weissman, J.S. (2004). Conformational variations in an infectious protein determine prion strain differences. Nature *428*, 323–328.

Tarczewska, A., and Greb-Markiewicz, B. (2019). The significance of the intrinsically disordered

regions for the functions of the bHLH transcription factors. Int. J. Mol. Sci. *20*, 5306.

Taylor, J.P., Brown, R.H., Jr., and Cleveland, D.W. (2016). Decoding ALS: from genes to mechanism. Nature *539*, 197–206.

Treusch, S., Hamamichi, S., Goodman, J.L., Matlack, K.E., Chung, C.Y., Baru, V., Shulman, J.M., Parrado, A., Bevis, B.J., Valastyan, J.S., et al. (2011). Functional links between Abeta toxicity, endocytic trafficking, and Alzheimer's disease risk factors in yeast. Science *334*, 1241–1245.

Wickner, R.B. (1994). [URE3] as an altered URE2 protein: evidence for a prion analog in Saccharomyces cerevisiae. Science *264*, 566–569.

Wilcken, R., Wang, G., Boeckler, F.M., and Fersht, A.R. (2012). Kinetic mechanism of p53 oncogenic mutant aggregation and its inhibition. Proc. Natl. Acad. Sci. U S A *109*, 13584–13589.

Xu, J., Reumers, J., Couceiro, J.R., De Smet, F., Gallardo, R., Rudyak, S., Cornelis, A., Rozenski, J., Zwolinska, A., Marine, J.C., et al. (2011). Gain of function of mutant p53 by coaggregation with multiple tumor suppressors. Nat. Chem. Biol. *7*, 285–295.

Supplemental Information

Tumor suppressor protein p53 expressed

in yeast can remain diffuse, form a prion,

or form unstable liquid-like droplets

Sei-Kyoung Park, Sangeun Park, Christine Pentek, and Susan W. Liebman
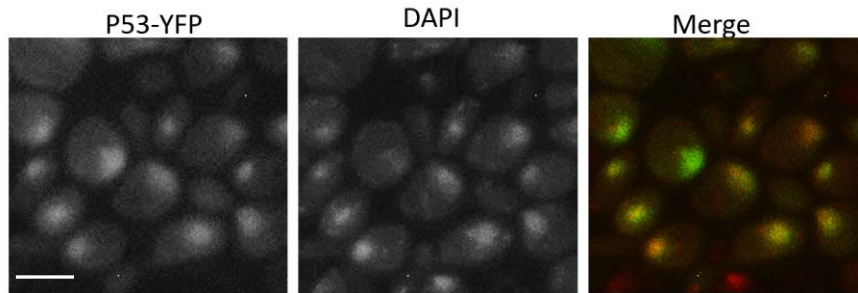
Supplemental Figures

Figure S1 (related to Figure 1). In non-prion cells, p53-YFP is diffuse in the nucleus. P53 is expressed constitutively from pGPD-p53-EYFP in strain yIG397. Cells were grown overnight on plasmid selective glucose media. Nuclei were stained with DAPI. Size bar indicates 5μM.
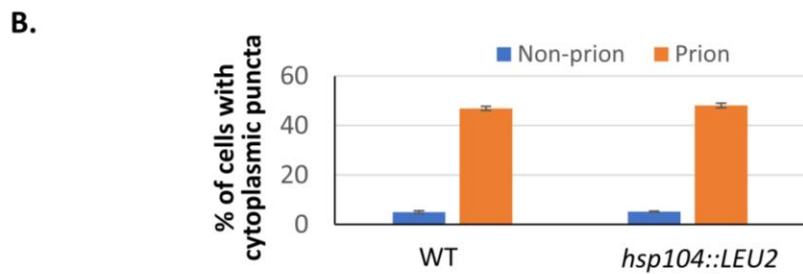
A.

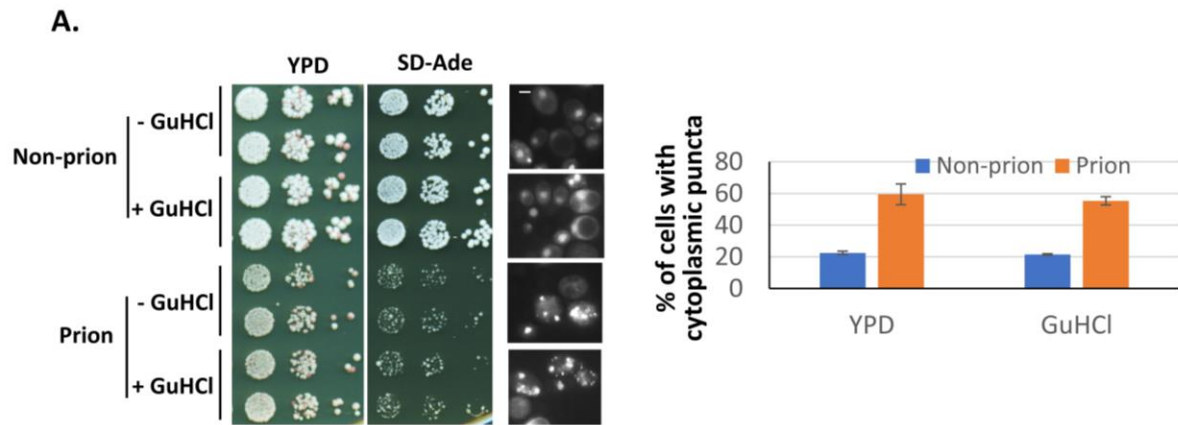**B.**

C.

D.

hsp104::kanMX4
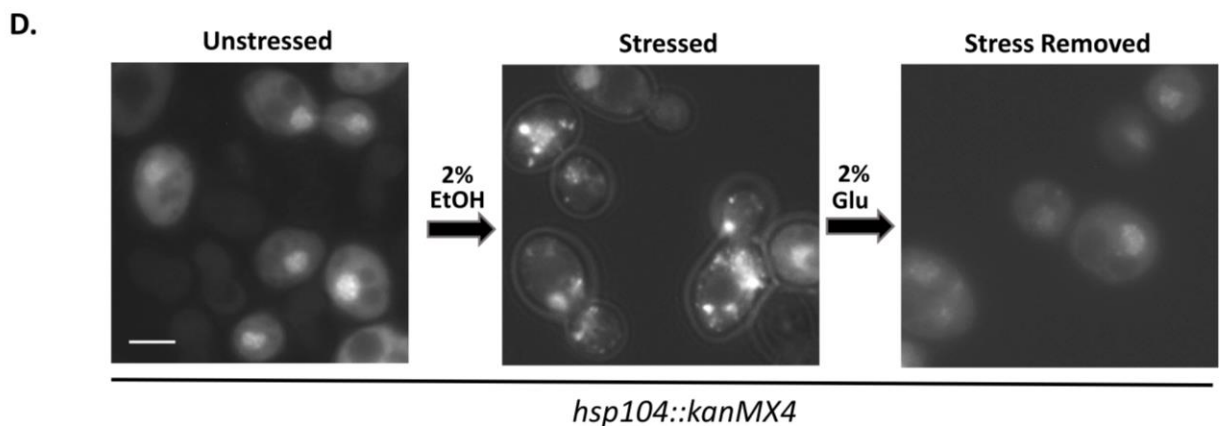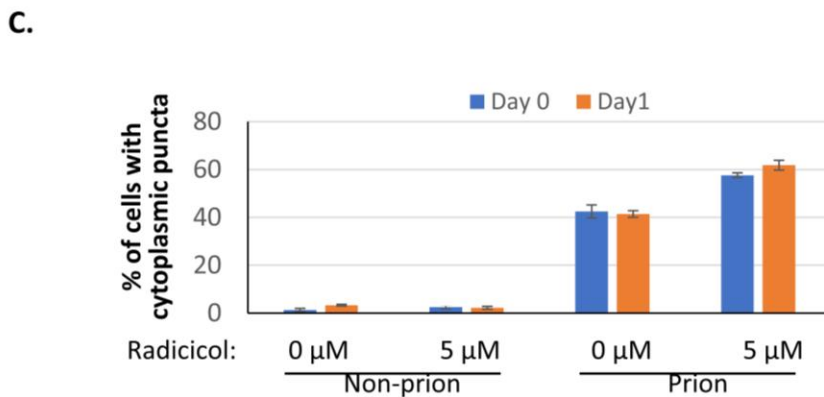
Figure S2. Chaperones tested have no effect on p53 prion retention or stress granule formation (related to Figures 1 and 5). *A. Growth in guanidine did not cause loss of the p53 prion.* Strain L3672 containing the p53 prion and its isogenic non-prion control (L3671) were streaked sequentially for 4 passages on YPD and YPD + 5mM GuHCl plates. Cells were then

normalized to OD_{600} =3, 1/10th serially diluted in water and spotted on complex glucose (YPD) and glucose -Ade (SD-Ade). Also shown are photographs of p53-EYFP fluorescence in cells and the percent of cells with cytoplasmic foci based on 6 replicates of 150-500 cells each with standard error of the mean. There was no statistical difference whether or not cells were grown on guanidine. B. Disruption of *HSP104 did not cause loss of the p53 prion. HSP104* was disrupted in cytoductants of L3663 transformed with *pGPD-p53-EYFP* containing the p53 prion as well as in isogenic controls lacking the p53 prions. The fraction of cells with cytoplasmic puncta was determined and plotted. Standard error of the mean bars shown were based on 3 replicates where 200-400 cells were scored for each replica. There was no statistical different whether or not *HSP104* was disrupted. *C. HSP90 is not required for p53 prion maintenance.* To test whether Hsp90 effects p53 prion propagation, prion (L3672) and isogenic non-prion control (L3671) cells were grown in complete glucose liquid media without or with 5 μM radicicol, a potent Hsp90 inhibitor. The percent of cells with nuclear diffuse and cytoplasmic p53-EYFP puncta are shown. The standard error of the mean bars are based on 3 replicates with 200-600 cells for each replica. *D. Stress droplets form even in the absence of HSP104.* Exponentially growing BY4741 *hsp104Δ* cells transformed with pGPD-p53-EYFP grown in plasmid selective glucose medium (unstressed) were resuspended in 2% ethanol medium for 1 hr (stressed) and then resuspended in glucose medium for 30 min (stress removed). Size bar indicates 5μM.
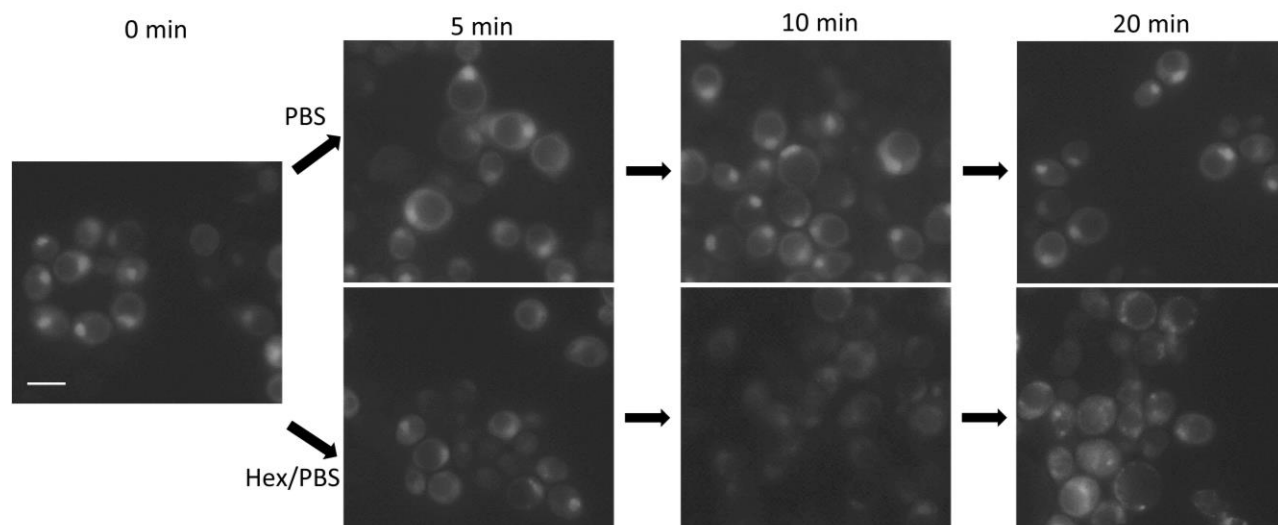
Figure. S3. 1,6-Hexanediol causes the appearance of wild type p53-EYFP cytoplasmic dots (related to Figure 5). yIG397 cells transformed with pGPD-p53-EYFP grown on glucose plasmid selective media were treated with 10% 1,6-hexanediol. Fluorescence was assayed at 5, 10 and 20 min. 1,6-Hexanediol induced p53 foci started to appear at 15 min and were plentiful by 20 min. Foci were not seen at either 5 or 10 min. Size bar indicates 5µM.

Transparent Methods

Yeast Strains, Plasmids, and Cultivation.

Media, cultivation and transformation procedures were standard (Sherman, 2002). Yeast with *ade2* mutations were maintained on complex glucose medium (YPD) supplemented with adenine (200 µg/ml) to prevent the appearance of *ade2* suppressors. Synthetic glucose media (SD) was supplemented with required amino acids. Strains and plasmids used are listed in Tables S1 and S2, respectively. The yeast strain used to assay for p53 activity and in which we selected the p53 prion was yIG397 (*MATα ade2-1 leu2-3,112 trp1-1 his3-11,15 can1-100, ura3-1 URA3 3xRGC::pCYC1::ADE2*) (kindly supplied by A. Inga, U of Trento, Italy) (Inga et al., 1997) (Flaman et al., 1995; Ishioka et al., 1993), with the integrated plasmid pLS210 (Flaman et al., 1995) that contains an *ADE2* reporter gene under three copies of the p53 consensus binding sequence from the ribosomal gene cluster (RGC) immediately upstream of minimal promoter CYC1 with a *URA3* selectable marker. Expression of *ADE2* was used to assay for p53 function in yIG397, L3671, L3672 and L3628 by analyzing growth and color of yeast by spotting 10X serially diluted suspensions of cells (initially normalized to $OD_{600} = 3$) on plasmid selective media with limiting adenine (5 µg/ml). When yIG397 was transformed with plasmids expressing wild type p53, it was prototrophic for adenine, yielding white colonies on plates containing a limited amount of adenine or YPD. Without functional p53, yIG397 is red and with limited p53 function it is pink. The non-prion control strain, L3671, was yIG397 co-transformed with pADH1-p53 and pGAL1-p53-EYFP. The prion strain induced in L3671 is L3672.

Strains L3719 and L3628 were used as recipients for transfection. L3719 and L3628 are a diploid strains we made by respectively selecting for *MAT**a**/MAT**a*** or *MATα/MATα* resulting from mitotic crossovers following low level UV irradiation of the *MAT**a**/MATα* strain SGY6001 (*MAT**a**/MATα lys-801/ lys-801 ade2-101/ ade2-101 trp1-Δ63/ trp1-Δ63 his3-Δ200/ his3-Δ200 leu2-Δ1/ leu2-Δ1 URA3::3xRGC::p-cyc1::ADE2::ura3-52/ ura3-52*) kindly provided by Samir K Maji, IIT, India (Sengupta et al., 2017, 2020). Strain L3663 (*MAT**a** kar1 ura2 his- leu2* [*PIN+*] [*rho⁻*]) was used as a recipient for cytoduction. It was made by inducing 3385, kindly supplied by R.B. Wickner, N.I.H. (Wickner, 1994), to become [*rho⁻*] by streaking on medium with ethidium bromide.

HSP104 was disrupted in cytoductants of L3663 transformed with *pGPD-p53-EYFP* containing the p53 prion as well as in isogenic controls lacking the p53 prions. As described previously (Zhou et al., 1999), the disruptions were obtained with the one-step gene replacement method (Rothstein, 1983) by transforming the prion and non-prion cytoductants with a purified *Pvu*I and *Hind*III fragment containing *HSP104::LEU2* isolated from plasmid pYABL5 (Chernoff et al., 1995)**.** The disruptions were verified by PCR as described previously (Zhou et al., 1999).

Plasmid pADH1-p53 (pLS76=pRS415, p*ADH1-p53, CEN LEU2*), which expresses human p53 cDNA under control of constitutive *ADH1* promoter, was kindly provided by Dr. Richard Iggo, Bergonie Cancer Institute, France (Inga et al., 1997). This plasmid was used to screen for p53 prion cells. Gateway cloning was used to construct plasmids with wild-type or R175H mutant p53 expression controlled by *GAL1 or GPD1.* Human p53 without a stop codon was PCR amplified from pLS76 or pLS40 (*pGAL-p53 R175H, CEN, TRP1*) (Inga et al., 1997) and cloned into pDONR221 using a BP reaction to build p2506 or p2516 (respectively, pDONR221-p53 and pDONR221-p53mt R175H without stop codons). The p53 fragments in the entry clones were then transferred to p2258 (pAG414 *GAL1-ccdB-EYFP, TRP1, CEN*) and p2474 (pAG413 *GPD-ccdB-EYFP, HIS3, CEN*) (Alberti et al., 2007) by an LR reaction to respectively build pGAL1-p53-EYFP (p2489=pAG414 *GAL1-p53-EYFP, TRP1, CEN*) and pGPD-p53-EYFP (p2517=pAG413, *GPD-p53-EYFP, HIS3, CEN*) or pGAL-p53-R175H-EYFP (p2518=pAG414 *GAL1-p53-R175H-EYFP, TRP1, CEN*). The p53 sequences in the destination clones were confirmed (Genomic Center, University of Nevada, Reno) and strain yIG397 transformed with pADH1-p53 (pLS76=pRS415, p*ADH1-p53, CEN, LEU2*) and pGAL1-p53-EYFP (p2489=pAG414 *GAL1-p53-EYFP, TRP1, CEN*) (L3671) was confirmed to be white on adenine limiting (5 µg/ml), plasmid selection media.

TABLE S1. Yeast strains used, related to Figures 1-6

Strains	Description	Reference
yIG397	*MATα ade2-1 leu2-3,112 trp1-1 his3-11,15 can1-100 URA3::3xRGC::p-cyc1::ADE2::ura3-1*	(Inga et al., 1997)
L3671	*yIG397* transformed with *pADH1-p53* (*LEU2*) and *pGAL1-p53-EYFP* (*TRP1*)	This study
L3672	L3671 with p53 prion	This study
3385	*MATa kar1 ura2 leu2 his3* [*PIN⁺*]	(Wickner, 1994)
L3663	[*rho⁻*] version of 3385	This study
L3719	*MATa/MATa lys2-801/lys2-801 ade2-101/ade2-101 trp1-Δ63/trp1-Δ63 his3-Δ200/his3-Δ200 leu2-Δ1/leu2-Δ1 URA3::3xRGC::p-cyc1::ADE2::ura3-52/ ura3-52*	This study
L3628	*MATα/MATα lys2-801/lys2-801 ade2-101/ade2-101 trp1-Δ63/trp1-Δ63 his3-Δ200/his3-Δ200 leu2-Δ1/leu2-Δ1 URA3::3xRGC::p-cyc1::ADE2::ura3-52/ ura3-52*	This Study
BY4741 hsp104Δ	*MATa his3Δ1 leu2Δ0 met15Δ0 ura3Δ0 hsp104Δ::KanMX4 deletion strain in BY4741 background*	(Winzeler et al., 1999)

TABLE S2. Plasmids used, related to Figures 1-6

Short Name, and SWL Laboratory Plasmid #	Original Plasmid Name/Description	Reference
pADH1-p53, pLS76	pADH1-p53 (*CEN, LEU2*)	(Inga et al., 1997)
p2258	pAG414-GAL-ccdB-EYFP (*CEN, TRP1*)	Addgene plasmid #14215
p2474	pAG413-*GPD-ccdB-EYFP* (*CEN, HIS3*)	Addgene plasmid #14214
pGAL-p53-EYFP, p2489	pGAL1-p53-EYFP (*CEN, TRP1*)	This study
pGPD-p53-EYFP, p2517	pGPD1-p53-EYFP (*CEN, HIS3*)	This study
pGPD-p53-R175H-EYFP, p2518	pGPD1-p53-R175H-EYFP (*CEN, HIS3*)	This study
pEdc3-mCH, p2137	pRP1575 Edc3-mCh (*CEN, TRP1*)	(Buchan et al., 2008)
pDcp2-RFP, p2136	pRP1155 Dcp2-RFP (*CEN, LEU2*)	(Teixeira et al., 2005)
p812	pYABL5, *HSP104::LEU2*	(Chernoff et al., 1995)

Selection for p53 Prion

L3671 was patched all over plasmid selective adenine limiting glucose plates. After robust growth these were velveteen replica-plated to each of 4 galactose and 4 glucose plasmid selective adenine limiting plates, where respectively p53-EYFP was, or was not, expressed. After 5 days incubation at 30°C each of these plates were replica-plated to glucose plasmid selective adenine limiting media to end the transient p53-EYFP overexpression caused by previous growth on galactose. Plates were grown for 3 days at 30°C. They were then transferred to room temperature for 3 weeks for further growth and to allow the development of the red/pink color diagnostic for cells with reduced *ADE2* expression expected of strains with p53 prion.

Induction and Removal of Stress
Cells transformed with pGPD-p53-EYFP (p2517) or pGAL-p53-R175H-EYFP (p2518) were grown to exponential phase in plasmid selective media. For ethanol stress, cells were washed twice with deionized water, resuspended and incubated with shaking for 30 min in plasmid selective 2% ethanol media and resuspended in plasmid selective glucose medium for stress removal. For heat stress, cells grown in plasmid selective glucose medium were incubated for 10 min in a 46˚C water bath before being returned to 30˚C. For glucose starvation, cells were washed twice with deionized water, resuspended in synthetic medium without any carbon source and incubated for 20 min with shaking. To remove glucose starvation stress, cells were harvested, resuspend in plasmid selective glucose medium and incubated for 20 min with shaking.

Sedimentation Analysis and Immuno-blotting
L3671 (non-prion control) and L3672 (prion) cells grown on dextrose or galactose plasmid selective media were harvested and lysed as described previously (Park et al., 2019). To compare levels of proteins in supernatant vs. pellet, normalized cleared cell lysates (150 μl of 100 μg of protein/ml) were centrifuged at 80,000 rpm for 30 min at 4°C. After the supernatant was removed and saved, pellets were washed with lysate buffer containing a protease inhibitor cocktail and PMSF protease inhibitor, recentrifuged at 80,000 rpm for 10 min and resuspended in 150 μl of lysate buffer with protease inhibitors. Boiled proteins in equal volumes total (T), supernatant (S) and pellet (P) fractions were resolved by PAGE that was immunoblotted with anti-p53 (DO-1, Santa Cruz Biotechnology, Santa Cruz CA). The blots were then stripped and reprobed with loading control anti-PGK (Novex, Thermo Fisher Scientific, Waltham, MA).

Fluorescence Microscopy, Thioflavin T Staining, DAPI Staining and 1,6-Hexanediol Treatment
To see EYFP labeled p53 aggregates in p53 prion subclones, cytoductants or transfectants, we examined cells taken from plates after 5 days growth at 30°C on plasmid selective galactose medium (for prion subclones with GAL1-p53-EYFP) or 3 days growth on plasmid selective glucose medium (for transfectants and cytoductants with GPD1-p53-EYFP). P53 cytoplasmic foci were also stained with ThT in fixed cells as in (Johnson et al., 2008). Visualization of EYFP labeled or ThT stained cytoplasmic p53 was done with a Nikon Eclipse E600 fluorescent microscope (100X oil immersion) equipped with FITC, YFP, mCH and CFP filter cubes. P53-EYFP was visualized in the YFP channel, and ThT was viewed in the CFP channel. Cells expressing EYFP that were fixed for ThT staining exhibited reduced EYFP fluorescence. Both mCH and RFP were viewed with an mCH filter. To visualize nuclei, cells were stained with 1 μ g/ml 40,60-diamidino-2- phenylindole (DAPI) in 1XPBS for 10 min after fixation for 1 hr with 4% paraformaldehyde and permeabilized for 30 min with 60% EtOH. To determine if p53 foci in cells had the property of being dissolved by the aliphatic alcohol, 1,6-hexanediol shown to dissolve liquid-like over solid-like assemblies (Kroschwald et al., 2017), prion cells or cells under stress conditions were suspended in 10% 1,6-hexanediol and 10 μg/ml digitonin for 5 min before examining them for foci.

Cytoduction
[*RHO*+] p53 prion strain L3672 or [*RHO*+] non-prion isogenic control L3671, respectively containing or not containing p53 prion aggregates, were mated with recipient, L3663 (*MAT**a** kar1 ura2 his3 leu2* [*PIN*+] [*rho*-]) transformed with pGPD-p53-EYFP (*CEN, HIS3*) or pGPD-p53-R175H-EYFP (*CEN, HIS3*) for about 8 hours until zygotes were visible. The mating mixtures were then spread on synthetic glucose medium lacking histidine (SD-His) to select for single colonies, that were then patched on a master plate (SD-His) and replicated onto YPGly (complete medium with 2% glycerol as the sole carbon source) media where recipients that were cytoduced (Conde and Fink, 1976) to become [*RHO*+], by gaining donor cytoplasm, can grow. Colonies picked from plasmid selective glucose media and confirmed to be *MAT**a** Ura- Leu- His+ were scored as cytoductants and examined under a fluorescent microscope to score for the presence or absence of EYFP foci.

In vitro Polymerization of P8 Peptide

Aggregation-prone p53-derived peptide, p8 (NH2-PILTIITL-COOH, purchased from GeneScript USA Inc. Piscataway, NJ) was dissolved in 0.5 ml of 5.0 % D-mannitol and 0.01% sodium azide (pH 5.5) at a concentration of 1 mM in 1.5 ml Eppendorf tubes and placed in a water bath sonicator at its maximum output for 3 cycles of 20 sec resulting in a clear solution (Ghosh et al., 2014). The peptide was polymerized at room temperature with mild shaking for 8 hours and polymerization was confirmed with a ThT binding assay: 2 μl of 1 mM of P8 was mixed with 2 μl of the 1mM ThT in Tris-HCl (pH 8.0) and the volume was adjusted with 5% D-mannitol and 0.01% sodium azide (pH5.5) to give a final peptide concentration of 50 μM before measuring the fluorescence with a spectrofluorometer (SpectraMax M5, Molecular Devices, San Jose, CA), with excitation 450 nm and an emission 460-500 nm (Naiki et al., 1989).

Preparation of Yeast Spheroplasts for Transfection with Cell Lysates or P8 Polymer

Transfection was as previously described (Tanaka et al. 2004). Crude cell lysate either from prion (L3672) or non-prion (L3671) p53 cells, or *in vitro* made P8 polymer, were co-transformed along with pGPD-p53-EYFP (*HIS3, CEN*), into a recipient lacking p53 (L3628). Prion and non-prion p53 cells were grown on plasmid selective glucose media (SD-Leu-Trp) for 2 days at 30°C. Harvested cells were then resuspended in STC buffer (1M sorbitol, 10 mM CaCl2, 10 mM Tris-HCl pH7.5) including 10 mM PMSF, and an anti-protease cocktail for yeast (Sigma, St. Louis, MO) and lysed by vortexing with glass beads. Cell debris was removed by centrifugation 2X at 4°C for 5 min at 8,000 g. The clear cell-free lysates or polymer of P8 were sonicated (output 4) for 30 seconds 3X using a micro tip (Misonix XL-2000 Misonix Inc. Farmingdale, NY). Fresh spheroplasts of recipient strain L3628 were obtained using lyticase and maintained in STC buffer at 4°C and were mixed with sonicated lysates or polymer of P8 along with pGPD-p53-EYFP (*HIS3, CEN*) (20 μg/ml) and salmon sperm DNA (100 μg/ml). After heat shock in the presence of 25% PEG 3350 the spheroplasts were incubated in SOS (1M sorbitol, 0.3 YPD, 10 mM CaCl$_2$) at 30°C and added to SD-His with limiting adenine agar medium supplemented with 1M sorbitol. This was then overlaid on SD-His plates and incubated at 30°C to select for transfectants. Transfectants confirmed to be His$^+$, Lys$^-$, Leu$^-$, and Trp$^-$, that therefore contained the pGPD-p53 -EYFP without plasmids from the donor, were assayed for the presence of p53-EYFP foci.

Supplemental References

Alberti, S., Gitler, A.D., and Lindquist, S. (2007). A suite of Gateway cloning vectors for high-throughput genetic analysis in Saccharomyces cerevisiae. Yeast *24*, 913-919.

Buchan, J.R., Muhlrad, D., and Parker, R. (2008). P bodies promote stress granule assembly in Saccharomyces cerevisiae. J Cell Biol *183*, 441-455.

Flaman, J.M., Frebourg, T., Moreau, V., Charbonnier, F., Martin, C., Chappuis, P., Sappino, A.P., Limacher, I.M., Bron, L., Benhattar, J.*, et al.* (1995). A simple p53 functional assay for screening cell lines, blood, and tumors. Proceedings of the National Academy of Sciences of the United States of America *92*, 3963-3967.

Ishioka, C., Frebourg, T., Yan, Y.X., Vidal, M., Friend, S.H., Schmidt, S., and Iggo, R. (1993). Screening patients for heterozygous p53 mutations using a functional assay in yeast. Nature genetics *5*, 124-129.

Johnson, B.S., McCaffery, J.M., Lindquist, S., and Gitler, A.D. (2008). A yeast TDP-43 proteinopathy model: Exploring the molecular determinants of TDP-43 aggregation and cellular toxicity. Proc Natl Acad Sci U S A *105*, 6439-6444.

Naiki, H., Higuchi, K., Hosokawa, M., and Takeda, T. (1989). Fluorometric determination of amyloid fibrils in vitro using the fluorescent dye, thioflavin T1. Anal Biochem *177*, 244-249.

Rothstein, R.J. (1983). One-step gene disruption in yeast. Methods Enzymol *101*, 202-211.

Sengupta, S., Maji, S.K., and Ghosh, S.K. (2017). Evidence of a Prion-Like Transmission of p53 Amyloid in Saccharomyces cerevisiae. Molecular and cellular biology *37*.

Sengupta, S., Maji, S.K., and Ghosh, S.K. (2020). Retraction for Sengupta et al., "Evidence of a Prion-Like Transmission of p53 Amyloid in Saccharomyces cerevisiae". Molecular and cellular biology *40*.

Sherman, F. (2002). Getting started with yeast. Methods Enzymol *350*, 3-41.

Teixeira, D., Sheth, U., Valencia-Sanchez, M.A., Brengues, M., and Parker, R. (2005). Processing bodies require RNA for assembly and contain nontranslating mRNAs. RNA *11*, 371-382.

Winzeler, E.A., Shoemaker, D.D., Astromoff, A., Liang, H., Anderson, K., Andre, B., Bangham, R., Benito, R., Boeke, J.D., Bussey, H*., et al.* (1999). Functional characterization of the S. cerevisiae genome by gene deletion and parallel analysis. Science *285*, 901-906.

Zhou, P., Derkatch, I.L., Uptain, S.M., Patino, M.M., Lindquist, S., and Liebman, S.W. (1999). The yeast non-Mendelian factor [ETA+] is a variant of [PSI+], a prion-like form of release factor eRF3. EMBO J *18*, 1182-1191.